

1 **Infant milk formula produced by membrane filtration promotes mucus production in**  
2 **the upper small intestine of young pigs**

3

4 Cathal A. DOLD<sup>a,b</sup>, Simona L. BAVARO<sup>c</sup>, Yihong CHEN<sup>a</sup>, Michael J. CALLANAN<sup>d</sup>,  
5 Deirdre KENNEDY<sup>a</sup>, Joe CASSIDY<sup>e</sup>, John TOBIN<sup>a</sup>, Aylin W. SAHIN<sup>b</sup>, Peadar G.  
6 LAWLOR<sup>f</sup>, André BRODKORB<sup>a</sup> and Linda GIBLIN<sup>a,\*</sup>

7

8 <sup>a</sup>Teagasc Food Research Centre, Moorepark, Fermoy, Co. Cork, P61 C996, Ireland

9 <sup>b</sup>School of Food and Nutritional Sciences, University College Cork, Cork, T12 CY82, Ireland

10 <sup>c</sup>ISPA-CNR, Institute of Sciences of Food Production of National Research Council of Italy,  
11 Via Provinciale Lecce-Monteroni, 73100 Lecce, Italy

12 <sup>d</sup>Department of Biological Sciences, Munster Technological University, Cork, T12 P928  
13 Ireland

14 <sup>e</sup>School of Veterinary Medicine, Veterinary Science Centre, University College Dublin,  
15 Belfield, Dublin 4, Ireland

16 <sup>f</sup>Pig Development Department, Teagasc Animal and Grassland Research and Innovation  
17 Centre, Moorepark, Fermoy, Co. Cork, P61 C996, Ireland

18

19 **\*Corresponding Author:** Linda GIBLIN ([linda.giblin@teagasc.ie](mailto:linda.giblin@teagasc.ie)) (Tel: +3532542614)

20

21 **Abbreviations:** IMF, infant milk formula; UHT, ultra-high temperature; MEM, membrane  
22 filtration; HT, high-temperature; CML, N (6)-carboxymethyllysine; RPLP0, ribosomal  
23 protein lateral stalk subunit P0; XLD, Xylose Lysine Deoxycholate; VRBGA, Violet Red  
24 Bile Glucose Agar; TSA, Tryptic Soy Agar; MUC-1, mucin-1; MUC-2, mucin-2; CLDN-1,  
25 claudin-1; CLDN-2, claudin-2; CLDN-4, claudin-4; OCLN, occludin; ZO-1, zona occludens-

26 1; JAM-A, junctional adhesion molecule A; RAGE, receptor for advanced glycation end  
27 products; IL-6, interleukin 6; IL-8, interleukin 8; TNF- $\alpha$ , tumor necrosis factor alpha; PBS,  
28 phosphate buffered saline; cDNA, complementary DNA; BCA, bicinchoninic acid; WPC,  
29 whey protein concentrate.

30 **Abstract:**

31 Human breast milk promotes maturation of the infant gastrointestinal barrier, including the  
32 promotion of mucus production. In the quest to produce next generation infant milk formula  
33 (IMF), we have produced IMF by membrane filtration (MEM-IMF). With a higher quantity  
34 of native whey protein, MEM-IMF more closely mimics human breast milk than IMF  
35 produced using conventional heat treatment (HT-IMF). After a 4-week dietary intervention in  
36 young pigs, animals fed a MEM-IMF diet had a higher number of goblet cells, acidic mucus  
37 and mucin-2 in the jejunum compared to pigs fed HT-IMF ( $P < 0.05$ ). In the duodenum,  
38 MEM-IMF fed pigs had increased trypsin activity in the gut lumen, increased mRNA  
39 transcript levels of *claudin 1* in the mucosal scrapings and increased lactase activity in brush  
40 border membrane vesicles than those pigs fed HT-IMF ( $P < 0.05$ ). In conclusion, MEM-IMF  
41 is superior to HT-IMF in the promotion of mucus production in the young gut.

42

43 **Keywords:** Infant milk formula; membrane filtration; goblet cells; digestive enzymes; gut  
44 barrier.

45 **Highlights:**

- 46 • Infant milk formula processing alters intestinal and mucosal barrier biomarkers
- 47 • Membrane filtration processing increases goblet cell number and mucus secretion
- 48 • Membrane filtration processing increases key digestive and brush borders enzymes

49

## 50 **1. Introduction**

51 At birth, the human gastrointestinal tract is underdeveloped with lower levels of digestive  
52 enzymes and less uniform mucus in the gut barrier than the adult (Demers-Mathieu, 2022; Neu,  
53 2007). The undeveloped functionality of the infant gastrointestinal tract at birth increases the  
54 risk of infections which may result in necrotising enterocolitis (Renz, Brandtzaeg, & Hornef,  
55 2011). Nutritional strategies implemented with new-born infants have a major influence on  
56 gastrointestinal development and maturity (Neu, 2007). Human breast milk is proven to be  
57 easier to digest and, promotes gastrointestinal maturity, gut microbiota diversity and  
58 production of mucus from goblet cells (Dimitroglou et al., 2022). When breast milk is  
59 unavailable, infant formula is the alternative (Bookhart et al., 2021; Phosanam, Chandrapala,  
60 Huppertz, Adhikari, & Zisu, 2021). Infant milk formula (IMF) recipes are traditionally bovine  
61 milk based and must have a minimum protein quantity of 1.8 g/100 kcal to be classified as an  
62 IMF (Codex-Alimentarius, 1981).

63 Unlike human breast milk, which by nature, is unprocessed, IMFs and it's ingredients routinely  
64 undergo high-thermal processing to ensure microbial safety (Wada & Lönnerdal, 2015).  
65 Regardless of processing systems, a heating step is introduced where the IMF liquid is spray  
66 dried to produce powders for extended shelf life and worldwide distribution. Extreme thermal  
67 loads imposed throughout production results in native protein denaturation, protein aggregation  
68 and formation of advanced glycation end products (Lund, Bechshøft, Ray, & Lund, 2021).

69 Thermal processing of IMF influences digestion kinetics. When examined *in vitro*, Ye et al.  
70 (2021) found increased protein aggregation and decreased protein digestibility in ultra-high  
71 temperature (UHT) IMF compared to lower heat treated IMF (Ye et al., 2021). Indeed, high  
72 temperature processing has been shown to reduce digestive and brush border membrane  
73 enzyme activities in rat (Wang & Zhao, 2021) and pig studies (Yanqi Li et al., 2018; Sun et al.,

74 2022). Heat treatment of IMF also negatively impacts on intestinal morphology, integrity and  
75 health *in vitro* and *in vivo* (Bavaro et al., 2021; Yanqi Li et al., 2018; Y. Li et al., 2013; Navis,  
76 Muncan, et al., 2020; Navis, Schwebel, et al., 2020; Sun et al., 2022).

77 Alternative membrane filtration processing systems have been utilised in recent studies to  
78 produce IMF powders with a reduced thermal load (Yihong Chen et al., 2021; Yu et al., 2021).  
79 Yu et al. (2021) produced IMF powders using membrane filtration. This IMF powder had  
80 significantly lower whey protein denaturation compared to an IMF produced using multiple  
81 heating steps ( $6 \pm 4\%$  vs  $58 \pm 0\%$ ) ( $P < 0.05$ ) (Yu et al., 2021). Recently, we produced an IMF  
82 powder by membrane filtration (MEM-IMF) using 1.4 and 0.2  $\mu\text{m}$  membranes (Yihong Chen  
83 et al., 2023). The native whey protein quantity in MEM-IMF was 59.9 % (Yihong Chen et al.,  
84 2023). There was a significantly lower amount of native whey protein (4.5 %) present in an  
85 IMF produced by conventional heat treatment (HT-IMF) ( $P < 0.001$ ) (Yihong Chen et al.,  
86 2023). In both studies, after spray drying, there was no significant differences in N (6)-  
87 carboxymethyllysine (CML) levels ( $3.65 \pm 0.74$  ng/mg IMF powder in MEM-IMF and  $3.97 \pm$   
88  $0.70$  ng/mg IMF powder in HT-IMF) in IMF powders produced by membrane filtration  
89 compared to high temperature processing (Yihong Chen et al., 2021; Yu et al., 2021).

90 *In vitro*, using a semi-dynamic model of the infant gut, the digestive behaviour in the gastric  
91 phase differed between MEM-IMF and HT-IMF (Y. Chen, Callanan, Giblin, Tobin, &  
92 Brodkorb, 2022). MEM-IMF had a fragmented curd and a quicker (93 min) dissociation of  
93 protein aggregates from fat droplets compared to HT-IMF, which had a firmer, larger curd with  
94 protein aggregates still visible on fat droplets at 156 min (Y. Chen et al., 2022). In young pigs,  
95 an MEM-IMF diet resulted in significantly higher levels of protein hydrolysis in the duodenum  
96 compared to the duodenum of pigs fed HT-IMF ( $P < 0.05$ ) (Yihong Chen et al., 2023). There  
97 was a significantly higher concentration of water soluble peptide/protein content in the jejunum

98 of pigs fed a MEM-IMF diet compared to pigs fed a HT-IMF diet ( $P < 0.001$ ), due to higher  
99 levels of 10 - 18 kDa, 18 - 28 kDa and 28 - 65 kDa molecular mass groups ( $P < 0.05$ ) (Yihong  
100 Chen et al., 2023). Interestingly, using an *in vitro* gut barrier model, simulated gastro-intestinal  
101 digested MEM-IMF was also found to increase barrier integrity and levels of tight junction  
102 protein claudin-1 (CLDN-1) (Bavaro et al., 2021).

103 The objective of this follow-up study was to investigate if a diet formulated with MEM-IMF  
104 resulted in digestive enzyme activity differences in the duodenum and jejunum of these young  
105 pigs that coincided with our observations of faster protein digestion kinetics. In addition, the  
106 study investigated whether or not membrane filtration processing altered gut physiology, for  
107 example mucus secretion or gut barrier structure in the young pigs. The hypothesis was that  
108 MEM-IMF will increase digestive capability and support gut barrier health in the upper small  
109 intestine.

110

## 111 **2. Materials and Methods**

### 112 **2.1. Materials**

113 Xylose Lysine Deoxycholate (XLD) Agar, Listeria Selective Oxford Agar and Violet Red Bile  
114 + Glucose Agar (VRBGA) were purchased from Oxoid (Ireland). The RNeasy Mini RNA  
115 extraction kit and DNase digestion kit were obtained from Qiagen (Germany). Oligonucleotide  
116 primers for reverse transcription quantitative real-time PCR (RT-qPCR) analysis were  
117 synthesised by Eurofins Genomics (Germany). The LightCycler 480 SYBR Green I Master  
118 was purchased from Roche Diagnostics (Germany). RIPA buffer, 1% EDTA and 1% Halt  
119 Protease Inhibitor Cocktail were purchased from Thermo Fisher Scientific (USA). The primary  
120 mucin-2 (MUC-2) polyclonal antibody (Cat. No. PA5-119292) was purchased from Invitrogen  
121 (USA). The housekeeping  $\beta$ -Actin polyclonal antibody (Cat. No. bs-0061R) was obtained from

122 Bioss Antibodies (USA). The Trans-Blot Turbo Transfer System containing PVDF membranes  
123 was purchased from Bio-Rad (USA). All other reagents were purchased from Sigma Aldrich  
124 (Ireland).

## 125 **2.2. Infant milk formula preparation and manufacturing**

126 A detailed description and schematic diagram of IMF processing was previously reported by  
127 Chen et al. (2021) (Yihong Chen et al., 2021). Briefly, the IMFs used in this trial were  
128 manufactured at pilot-plant scale based on the recommendations for first stage IMF (infant's  
129 aged < six months). Raw bovine whole milk was collected from the dairy farm at the Teagasc,  
130 Animal and Grassland Research and Innovation Centre Moorepark (Ireland). Both IMFs were  
131 manufactured in Moorepark Technology Limited (Ireland). Both IMFs had identical  
132 ingredients with protein: lactose: fat content of 1.29: 7: 3.49. The IMF had a whey:casein  
133 protein ratio of 60:40. MEM-IMF and HT-IMF were produced separately in a single batch. To  
134 reduce heat treatment, milk was not pasteurised prior to processing of MEM-IMF. The  
135 formulation was filtered using 1.4 and 0.2 µm filtration membranes. Only the microfiltration  
136 retentate from the 0.2 µm filtration membrane was heated at 80 °C for 30 s and 125 °C for 5 s.  
137 HT-IMF was pre-heated at 80 °C for 30 s before final heating at 125 °C for 5 s. Both IMFs  
138 were homogenised at 15 MPa and spray dried at inlet and outlet temperatures of 185 °C and 80  
139 °C, respectively. A total volume of 250 kg of each IMF powder was produced.

## 140 **2.3. Microbial analysis of infant milk formula powders**

141 Before inclusion in pig diets, microbial analysis of IMF powders was performed in accordance  
142 with Commission Regulation (EC) No 2073/2005 (Commission Regulation, 2005). In brief, 1  
143 g of IMF powder was added to 9 ml of Ringer's solution and serially diluted. Dilutions were  
144 plated (100 µl) on Tryptic Soy Agar (TSA), XLD Agar, Listeria Selective Oxford Agar,  
145 VRBGA and *Cronobacter spp.* ChromoSelect Agar, modified. Plates were incubated for 48 h

146 at 37 °C prior to plate counting. Microbial analysis of both IMF powders was performed in  
147 triplicate on different days.

#### 148 **2.4. Pig trial**

149 The pig trial was performed between June and August 2020, at the Teagasc Pig Development  
150 Department Moorepark (Ireland) (Yihong Chen et al., 2023). Ethical approval for this study  
151 was provided by the Teagasc Animal Ethics Committee (approval no. TAEC2020-248), and  
152 the project was sanctioned by the Health Products Regulatory Authority (project authorisation  
153 no. AE19132/P111). The experiment was performed in accordance with Irish legislation (SI  
154 no. 543/2012) and the EU Directive 2010/63/EU on the protection of animals used for scientific  
155 purposes. The health and welfare status of all animals was monitored daily throughout the  
156 duration of this study. Twenty (10 male and 10 female) recently weaned pigs [(Large White x  
157 Landrace; PIC Hermitage, Ireland) x Tempo; Topigs Norsvin; Premier Pig Genetics Ltd.,  
158 Ireland] were chosen for this study. At weaning ( $27 \pm 0.7$  days of age) pigs were blocked on  
159 the basis of sex, body weight ( $8.3 \pm 0.59$  kg) and litter origin. Within each block, pigs were  
160 randomly assigned to one of two dietary treatment groups ( $n = 10$ ) until 28 days post-weaning;  
161 (1) a starter diet containing 35 % of MEM-IMF or (2) a starter diet containing 35 % of HT-  
162 IMF. To meet the National Research Council nutrient requirements for pigs at weaning  
163 (National Research Council, 2012), a maximum of 35% inclusion of IMF powders was  
164 permitted. The ingredient and chemical composition of the starter diets were previously  
165 published by Chen et al. (2023) (Yihong Chen et al., 2023). The experimental diets were  
166 prepared to be both isonitrogenous and isocaloric. The pigs were individually penned in fully  
167 slatted pens (pen dimensions: 2.4 m x 1.8 m) and each pen was equipped with a single-spaced  
168 stainless steel feeder (30 cm wide; O'Donovan Engineering, Ireland) and a drinker bowl  
169 (BALP, France). From day 0 to 28 post-weaning, pigs were fed twice daily and access to water  
170 was on an *ad libitum* basis. All pigs remained healthy throughout the course of the trial.

## 171 **2.5. Slaughter and sample collection**

172 On day 28 post-weaning, 3 h after the pigs were given their final feed, they were humanely  
173 euthanized by captive bolt stunning and immediately exsanguinated. Following slaughter, gut  
174 lumen content was immediately collected from the duodenum (50 cm caudal to the pylorus)  
175 and jejunum (2.5 m caudal to the pylorus). The gut lumen content was snap frozen immediately  
176 in liquid nitrogen and stored at -80 °C until further analysis. The entire digestive tract was  
177 isolated and tissue from the duodenum (10 cm caudal to the pylorus) and jejunum (1.5 m caudal  
178 to the pylorus) were aseptically removed and gently rinsed with sterile phosphate buffered  
179 saline (PBS). For biochemical analysis, tissue samples were immediately snap frozen in liquid  
180 nitrogen and stored at -80 °C. For histological analysis, duodenal and jejunal tissue sections (2  
181 cm) were rinsed in PBS, placed in a No-Tox fixative solution (Cruinn Diagnostics Ltd, Ireland),  
182 stored at room temperature and then shipped on ice to NationWide Laboratories (UK) for  
183 mounting on glass microscope slides. To collect the mucosal scrapings, intestinal tissue  
184 sections (5 cm) were rinsed in PBS, cut longitudinally and the mucosa gently blotted dry with  
185 tissue paper. Using a glass microscopic slide, the muscularis layer was then removed and  
186 mucosal scrapings were immediately snap-frozen in liquid nitrogen and stored at -80 °C until  
187 analysis.

## 188 **2.6. Intestinal histology measurement and analysis**

189 Mounting of duodenal and jejunal tissue was performed as previously detailed by Crespo-  
190 Piazuelo et al. (2022) (Crespo-Piazuelo et al., 2022). In brief, fixed duodenal and jejunal tissue  
191 sections (2 cm) were removed from the No-Tox fixative solution and dehydrated through a  
192 graded alcohol series and cleared with xylene and embedded in paraffin wax. Tissue samples  
193 were cut finely into 5 µm sections using a microtome, mounted on glass microscope slides and

194 then stained with haematoxylin and eosin. Slides were coded to ensure measurements and  
195 analysis were performed without prior knowledge of treatment group.

196 For histological analysis, an Olympus BX51 Light Microscope (Olympus Corporation, Japan)  
197 equipped with a ProgRes CT3 camera (Jenoptik AG, Germany) was used in conjunction with  
198 ProgRes Capture Pro 2.10.00 software (Jenoptik AG, Germany). Mucosal thickness, villus  
199 height and crypt depth were measured using 10× objective magnification. For each pig, ten  
200 randomly selected, clearly identifiable villi and crypts were measured. Mucosal thickness was  
201 measured from the base of the mucosa to the tip of the villus. Villus height was then measured  
202 from the tip of the villus to its base. An associated crypt was then measured from the base of  
203 the villus to the base of the mucosa. For each villus measured, accompanying goblet cell  
204 numbers were counted using 40× objective magnification.

## 205 **2.7. Measurement of acidic mucins in mucus layer of pig small intestine using Alcian blue** 206 **dye**

207 To quantify acidic mucins, the procedure described previously by Smirnov et al. (2004)  
208 (Smirnov, Sklan, & Uni, 2004) was adopted, with slight modifications. Briefly, 50 mg tissue  
209 was defrosted on ice and submerged in 1% Alcian blue dye (1 ml) prepared in 160 mM sucrose,  
210 50 mM sodium acetate, pH 5.8. Following a 2 h incubation at 4 °C, excess dye was removed  
211 by rinsing the tissue in 250 mM sucrose. Subsequently, the absorbed Alcian blue dye was  
212 extracted from the tissue by incubation in 1 ml 500 mM magnesium chloride for a further 2 h  
213 at 4 °C. Samples were immediately centrifuged at 16000 × g for 20 min at 4 °C. The supernatant  
214 was retained for absorbance reading at 620 nm using a Synergy plate reader (BioTek, USA).  
215 The quantity of Alcian blue was determined using a standard curve of Alcian blue (0 - 250  
216 µg/ml). The results are reported as µg Alcian blue dye absorbed per mg tissue. Each  
217 measurement was performed with technical triplicates on two different days (n = 10 pigs).

## 218 **2.8. Analysis of mucin-2 expression by Western blot**

219 Mucosal scrapings were removed from -80 °C storage and thawed on ice. RIPA buffer (1 ml)  
220 in the presence of 1 % EDTA and 1 % Halt Protease Inhibitor Cocktail was added to 50 mg  
221 mucosal scraping. Total protein was then extracted from the mucosal scraping via  
222 homogenisation on ice with a T 25 ULTRA-TURRAX (IKA Works, Inc., USA). The  
223 homogenate was left agitating on ice for 2 h prior to centrifugation at 16000 × g for 20 min at  
224 4 °C to pellet excess debris. The supernatant was then collected, total protein content  
225 determined using the Pierce™ BCA Protein Assay Kit (Thermo Fisher Scientific, USA) and  
226 samples were stored at -80 °C for future analysis. Mucosal scraping protein extracts containing  
227 equal amounts of protein (25 µg) were separated by SDS-PAGE under reducing conditions  
228 using 4 – 15 % stain-free polyacrylamide gels at a constant voltage (100 V). SDS-PAGE gel  
229 was then transferred onto a PVDF membrane using the Trans-Blot Turbo Transfer System  
230 (Bio-Rad, USA).

231 The Western blotting protocol outlined in the WesternBreeze Chemiluminescent Western Blot  
232 Immunodetection Kit (Thermo Fisher Scientific, USA) was followed, with slight modifications.  
233 Separate, side-by-side, PVDF membranes were used for the target MUC-2 antibody and the β-  
234 actin housekeeping antibody. The membrane was initially blocked in blocking solution for 2 h  
235 at 4 °C to decrease non-specific binding. The membrane was then rinsed 3 times for 10 min  
236 with distilled water before being incubated with the primary antibody for MUC-2 (1:1500)  
237 overnight at 4 °C or the housekeeping antibody anti-β-actin (1:10000) diluted directly in  
238 blocking solution. The membrane was then washed 3 times for 10 min with antibody wash  
239 solution and then incubated for 2 h at 4 °C with the secondary IgG antibody. The membrane  
240 was exposed to the CDP-Star® chemiluminescent substrate (Thermo Fisher Scientific, USA)  
241 for 5 min. Immunoreactive proteins were visualised using the ChemiDoc XRS+ Gel Imaging  
242 System (Bio-Rad, USA). Densitometry analysis was undertaken with normalisation against the

243  $\beta$ -actin housekeeping antibody using Image Lab 6.1 software (Bio-Rad, USA). Western blots  
244 were performed in triplicate on two different days (n = 3 pigs).

## 245 **2.9. RNA extraction and complementary DNA synthesis**

246 Mucosal scrapings were removed from -80 °C storage and thawed on ice. RNA extraction was  
247 performed on 30 mg intestinal mucosal scraping using the RNeasy Mini Kit (Qiagen,  
248 Germany), according to the manufacturer's instructions, including the on-column DNase  
249 digestion step. Total RNA yields were quantified spectrophotometrically using the NanoDrop  
250 1000 Spectrophotometer (Thermo Fisher Scientific, USA). A quality control check to  
251 determine 260/280 absorbance ratios ensured only RNA samples with 1.8 - 2.1 ratios were  
252 used. RNA integrity was analysed by gel electrophoresis on a 1 % agarose gel (Bio-Rad, USA)  
253 in 1X TAE buffer at 130 V for 30 min. Reverse transcription from 700 ng RNA to  
254 complementary DNA (cDNA) was performed using the SensiFAST cDNA Synthesis Kit  
255 (Meridian Bioscience, USA) according to the manufacturers instructions. A sample containing  
256 no reverse transcription enzyme was also included as a negative control to track any genomic  
257 DNA contamination. cDNA synthesis was performed to a final volume of 20  $\mu$ l and stored at  
258 -20 °C.

## 259 **2.10. Quantification of mRNA transcript by reverse transcription quantitative real-time** 260 **PCR**

261 All tight junction and mucus secreting primers were designed to span intron-exon boundaries,  
262 where possible, using the Primer-BLAST software at the NCBI website  
263 (<http://www.ncbi.nlm.nih.gov/tools/primer-blast>) (Supplementary Table 1). Primers for  
264 *interleukin 6 (IL-6)*, *interleukin 8 (IL-8)* and *tumor necrosis factor alpha (TNF- $\alpha$ )* were  
265 obtained from Navis et al 2020a (Navis, Muncan, et al., 2020). RT-qPCR analyses was  
266 performed adhering to the MIQE guidelines (Bustin et al., 2009). For RT-qPCR, cDNA

267 samples were removed from -20 °C storage and thawed on ice. The annealing temperature for  
268 each individual primer pair was determined by running a real time quantitative temperature  
269 gradient from 55 to 65 °C. Primer amplification efficiencies were in the range 90 – 110 %  
270 determined by running a RT-qPCR with four different dilutions (1:1, 1:10, 1:100 and 1:1000)  
271 of cDNA. RT-qPCR was performed with a LightCycler® 96 instrument (Roche Diagnostics,  
272 Germany) and LightCycler 480 SYBR Green I Master kit. For each RT-qPCR run, 1 µl cDNA  
273 (1:10 dilution of cDNA synthesis reaction) and 0.5 µl of both forward and reverse primer (10  
274 µM) was added to 5 µl SYBR Green. The final reaction volume was brought to 10 µl using  
275 RNase free water. The thermal cycling protocol was performed as follows; 10 min pre-  
276 incubation at 95 °C, followed by 45 cycles of three step RT-qPCR with 10 s denaturation at 95  
277 °C, 10 s annealing at primer specific annealing temperature (55 - 63 °C) and extension at 72 °C  
278 for 30 s. A melting curve analysis was included with each RT-qPCR cycle to indicate single  
279 product melting and ensure no primer-dimers were present. A no-reverse transcription control  
280 sample and RNase free water sample were run with all RT-qPCR plates. The relative amount  
281 of target mRNA was determined using the reference gene, RPLP0. The relative mRNA  
282 expression was calculated using the  $2^{-\Delta\Delta C_t}$  method (Livak & Schmittgen, 2001). Data is  
283 presented as the fold changes compared to the HT-IMF (control) diet. Each RT-qPCR cycle  
284 was performed with technical duplicates on two different days (n = 7 pigs).

## 285 **2.11. Measurement of trypsin activity in the small intestine**

286 Trypsin activity (EC 3.4.21.4) in the gut lumen was determined using a commercial trypsin  
287 activity colorimetric assay kit (Trypsin Activity Colorimetric Assay Kit MAK290, Sigma-  
288 Aldrich, USA) using p-nitroaniline as a substrate, according to the manufacturer's instructions,  
289 with some slight modifications. Briefly, the gut lumen samples were defrosted on ice and  
290 centrifuged at  $14000 \times g$  for 10 min at 4°C to obtain a clear supernatant. Total protein content  
291 was determined spectrophotometrically at 562 nm using the Pierce™ BCA Protein Assay Kit

292 (Thermo Fisher Scientific, USA) on the collected supernatant, according to the manufacturers  
293 protocol (Supplementary Figure 1). Aliquots (200  $\mu$ l) of the supernatant were prepared, to limit  
294 freezing and thawing of samples, and diluted (1:200) in trypsin assay buffer for the enzyme  
295 assay. To 50  $\mu$ l of this diluted gut lumen sample, 50  $\mu$ l p-nitroaniline in trypsin assay buffer  
296 was added. The initial (T = 0 min) absorbance of the reaction was measured using a Synergy  
297 plate reader (BioTek, USA) at 405 nm. The final (T = 20 min) absorbance was again measured  
298 at 405 nm while still in the linear range of the reaction. A standard curve of p-nitroaniline (0 –  
299 40 nmol) was also prepared. One unit of trypsin activity was defined as the amount of enzyme  
300 causing the formation of one  $\mu$ mol of p-nitroaniline per min at 25°C. Trypsin activity was  
301 expressed as mU/mg total protein. Trypsin activity was measured with technical triplicates on  
302 two different days (n = 9 pigs).

## 303 **2.12. Isolation and purification of brush border membrane vesicles from pig small** 304 **intestine**

305 Intestinal brush border membrane vesicles were isolated and purified from duodenal and  
306 jejunal mucosal scrapings according to the protocol described by Mamone and Picariello  
307 (2023) (Mamone & Picariello, 2023). Briefly, 500 mg mucosal scrapings were thawed in 10  
308 ml ice-cold 50 mM mannitol, 2 mM Tris-HCl, pH 7.1. The mucosal scraping was then  
309 homogenized on ice with a T 25 ULTRA-TURRAX (IKA Works, Inc., USA). MgCl<sub>2</sub> (500  
310 mM) was then added to the homogenate to reach a final concentration of 10 mM. The  
311 suspension was agitated for 20 min at 4°C. Centrifugation at 2500  $\times$  g for 15 min at 4°C was  
312 performed to remove excess cell debris, basolateral, membranes, nuclei and mitochondria. The  
313 supernatant was then collected and ultra-centrifuged at 26000  $\times$  g for 30 min at 4°C using an  
314 ultracentrifuge (Beckman Coulter, USA). The supernatant was discarded and the pellet was  
315 retained. To further purify the brush border membrane vesicles, the pellet was again  
316 resuspended in 10 ml ice-cold 50 mM mannitol, 2 mM Tris-HCl, pH 7.1 and both

317 centrifugation steps were repeated. The final pellet was resuspended in 6 ml of 300 mM  
318 mannitol, 0.1 mM MgSO<sub>4</sub>, and 2 mM Tris, pH 7.4. To obtain a clear protein solution, the final  
319 suspension was passed several times through a 27-gauge needle. The isolated brush border  
320 membrane vesicles were snap-frozen in liquid nitrogen and stored in aliquots at -80 °C for  
321 future analysis. The Pierce™ BCA Protein Assay Kit (Thermo Fisher Scientific, USA) was  
322 used to determine the total protein content in the purified brush border membrane vesicles  
323 (Supplementary Figure 2).

### 324 **2.13. Determination of brush border membrane enzymatic activity in purified brush** 325 **border membrane vesicles from the pig small intestine**

326 Brush border membrane vesicles were removed from -80 °C storage and defrosted on ice.  
327 Brush border membrane enzyme activities were determined spectrophotometrically using  
328 enzyme-specific substrates in a Synergy plate reader (BioTek, USA) at the respective  
329 absorbance. A standard curve of known concentrations of each respective substrate was also  
330 prepared and absorbance measured at specific wavelength. All brush border membrane enzyme  
331 activities were expressed per mg cellular protein content of brush border membrane vesicles.  
332 Aminopeptidase N (EC 3.4.11.2) activity was determined using l-leucine p-nitroaniline  
333 substrate in 50 mM sodium phosphate buffer, pH 7.2 at 37 °C. Undiluted brush border  
334 membrane vesicle (10 µl) was added to each well and mixed with 190 µl sodium phosphate  
335 buffer (50 mM), pH 7.2 and l-leucine p-nitroaniline substrate. The liberated p-nitroaniline was  
336 measured at 405 nm. One unit of aminopeptidase N activity was defined as the amount of  
337 enzyme that catalyses the conversion of one µmol of p-nitroaniline per minute at pH 7.2 at 37  
338 °C. Aminopeptidase N activity was expressed as U/mg protein. Aminopeptidase A (EC  
339 3.4.11.7) activity was assayed using L-glutamic acid 1-(4-nitroanilide) as substrate in 50 mM  
340 sodium phosphate buffer, pH 8 at 37 °C. Undiluted brush border membrane vesicle (10 µl) was  
341 added to each well and mixed with 190 µl sodium phosphate buffer (50 mM), pH 8. The amount

342 of p-nitroaniline released was measured at 405 nm. One unit of aminopeptidase A activity was  
343 expressed as the amount of enzyme that catalyses the formation of one  $\mu\text{mol}$  of p-nitroaniline  
344 per minute at pH 8 at 37°C. Aminopeptidase A activity was expressed as mU/mg protein.  
345 Intestinal alkaline phosphatase activity (EC 3.1.3.1) was determined using p-nitrophenyl  
346 phosphate as a substrate using a colorimetric assay kit (Alkaline Phosphatase Activity  
347 Colorimetric Assay Kit BN00665, AssayGenie, Ireland), according to the manufacturer's  
348 protocol. In brief, 80  $\mu\text{l}$  diluted (1:100) brush border membrane vesicle was added to each well  
349 and mixed with 50  $\mu\text{l}$  assay buffer and p-nitrophenyl phosphate substrate. The liberated p-  
350 nitrophenol was measured at 405 nm. One unit of intestinal alkaline phosphatase activity was  
351 defined as the amount of enzyme that causes the formation of one  $\mu\text{mol}$  of p-nitrophenyl  
352 phosphate per minute at pH 9.6 and 25 °C. Intestinal alkaline phosphatase activity was  
353 expressed as U/mg protein. Lactase (EC 3.2.1.108) activity was analysed according to the  
354 protocol described previously by Dahlqvist et al. (1984) (Dahlqvist, 1984), with minor  
355 adjustments. Briefly, 50  $\mu\text{l}$  brush border membrane vesicle extracts were incubated for 60 min  
356 at 37 °C at a ratio of 1:1 with 50  $\mu\text{l}$  lactose (56 mM) in 100 mM Na-maleate, pH 6. The liberated  
357 glucose was then measured at 510 nm using the glucose oxidase assay kit (Glucose Oxidase  
358 Assay Kit K-GLOX, Megazyme, Ireland), according to manufacturer's instructions. Lactase  
359 activity was expressed as nmol of glucose/mg protein. One unit of lactase activity was defined  
360 as the amount of enzyme causing the formation of one  $\mu\text{mol}$  of glucose per minute at 37 °C.  
361 Each brush border membrane enzyme activity was measured with technical triplicates on two  
362 different days (n = 7 pigs).

#### 363 **2.14. Statistical Analysis**

364 All data are reported as means  $\pm$  standard error of the mean (SEM) of at least three or more  
365 biological replicates. Statistical analysis was performed using IBM SPSS Statistics Version 27

366 (IBM Statistics, USA). Results were regarded as statistically significant when  $P \leq 0.05$  and  
367 considered as tendencies at  $0.05 < P < 0.10$ .

368

### 369 **3. Results**

370 Microbial analysis of IMF powders produced at pilot plant scale, revealed that both IMFs met  
371 the microbiological safety requirements for IMFs outlined under Commission Regulation (EC)  
372 No 2073/2005 (Commission Regulation, 2005). Neither *Cronobacter sakazakii* nor *Salmonella*  
373 spp were detected in either powder. Although both powders had low levels of total bacterial  
374 counts, it was noted that MEM-IMF powder had significantly higher total bacterial counts  
375 compared to HT-IMF powder ( $1.8 \times 10^7$  vs  $8.3 \times 10^2$  CFU/g powder) ( $P < 0.05$ ). To meet the  
376 National Research Council nutrient requirements for pigs at weaning (National Research  
377 Council, 2012), a maximum inclusion of 35% of IMF powders was permitted in the starter diet.  
378 The post-weaning growth performance of pigs fed either MEM-IMF diet or HT-IMF diet has  
379 been previously described by Chen et al. (2023) (Yihong Chen et al., 2023). In brief, over the  
380 28 day trial, pigs in both treatment groups had similar average daily gain, average daily feed  
381 intake and feed conversion efficiency ( $P > 0.05$ ). Body weight of pigs was not affected by IMF  
382 treatment ( $P > 0.05$ ).

#### 383 **3.1. Measurement of trypsin activity in the small intestine**

384 As protein digestion kinetics in the upper gastrointestinal tract were faster in MEM-IMF fed  
385 pigs compared to pigs fed HT-IMF diets (Yihong Chen et al., 2023), trypsin activities were  
386 measured in the gut lumen collected from the duodenum and jejunum of pigs 3 h after their  
387 final feed (Figure 1). Pigs fed MEM-IMF diet had significantly higher trypsin activity in the  
388 duodenum than pigs fed HT-IMF diet ( $1.36 \pm 0.19$  mU/mg protein vs  $0.91 \pm 0.20$  mU/mg  
389 protein) ( $P < 0.05$ ). There were no differences in trypsin activity in the jejunum of pigs fed

390 either IMF ( $P > 0.05$ ). Pigs fed MEM-IMF diet tended to have higher trypsin activity in the  
391 duodenum ( $1.36 \pm 0.19$  mU/mg protein) compared to the jejunum ( $1.01 \pm 0.09$  mU/mg protein)  
392 ( $P < 0.10$ ). There was no difference in trypsin activity in the duodenum and jejunum in pigs  
393 fed HT-IMF diet ( $P > 0.05$ ).

### 394 **3.2. Influence of processing on brush border membrane enzymatic activity**

395 To investigate if IMF processing altered brush border membrane enzymatic activities,  
396 aminopeptidase N, aminopeptidase A, intestinal alkaline phosphatase and lactase activity were  
397 determined in the isolated brush border membrane vesicles (Table 1). These vesicles were  
398 extracted from mucosal scrapings collected from the pigs' upper small intestine. In the  
399 duodenal brush border membrane, a significantly lower aminopeptidase N activity was  
400 detected in pigs fed MEM-IMF diet versus HT-IMF fed pigs ( $5.23 \pm 0.26$  U/mg protein vs  $7.44$   
401  $\pm 0.69$  U/mg protein) ( $P < 0.05$ ). Overall, the total aminopeptidase N activity in the brush  
402 border membrane of the duodenum and jejunum had a tendency to be lower in MEM-IMF fed  
403 pigs compared to HT-IMF fed pigs ( $P < 0.10$ ). There was a significant increase in lactase  
404 activity in the brush border membrane of the duodenum of MEM-IMF fed pigs compared to  
405 HT-IMF fed pigs ( $166.59 \pm 22.09$  nmol of glucose/mg protein vs  $110.75 \pm 7.21$  nmol of  
406 glucose/mg protein) ( $P < 0.05$ ). No significant differences were observed in lactase activity  
407 between treatments in the jejunum. Processing did not influence aminopeptidase A and  
408 intestinal alkaline phosphatase activity in the small intestine brush border membrane, with no  
409 significant differences detected between treatment groups ( $P > 0.05$ ). Interestingly, the  
410 aminopeptidase N activity in the brush border membrane of MEM-IMF pigs increased the  
411 further down the intestinal tract ( $5.23 \pm 0.26$  U/mg protein in the duodenum vs  $6.59 \pm 0.47$   
412 U/mg protein in the jejunum) ( $P < 0.05$ ). There was no significant differences in  
413 aminopeptidase N activity in brush border membranes between duodenum and jejunum for  
414 HT-IMF fed pigs ( $P > 0.05$ ). Duodenal brush border membrane aminopeptidase A activity was

415 significantly higher than the jejunum for both MEM-IMF and HT-IMF fed pigs ( $P < 0.05$ ).  
416 Increased brush border membrane lactase activity was observed in the HT-IMF group in the  
417 jejunum ( $168.45 \pm 18.04$  nmol of glucose/mg protein) compared to the duodenum ( $110.75 \pm$   
418  $7.21$  nmol of glucose/mg protein) ( $P < 0.05$ ).

### 419 **3.3. Effects of IMF processing on small intestinal/gut physiology of pigs**

420 To investigate if IMF processing altered gut barrier physiology, mucosa thickness, villus  
421 height, crypt depth and goblet cell numbers, histological analysis was performed on the  
422 duodenum and jejunum of pigs fed MEM-IMF or HT-IMF diets (Table 2, Supplementary  
423 Figures 3 and 4). Pigs fed MEM-IMF diet had a significantly higher number of goblet cells in  
424 the jejunum ( $17.39 \pm 1.43$ ) compared to pigs on the HT-IMF diet ( $11.7 \pm 1.27$ ) ( $P < 0.05$ ). No  
425 significant difference in goblet cells numbers were observed between treatment types in the  
426 duodenum. Processing type had no significant effect on duodenal or jejunal villus height, crypt  
427 depth or villus height: crypt depth ratio. However, significant differences were noted within  
428 treatment type between intestinal regions. There were significantly higher number of goblet  
429 cells in the duodenum compared to the jejunum in both IMF treatments (MEM-IMF ( $27.98 \pm$   
430  $3.56$  vs  $17.39 \pm 1.43$  ( $P < 0.05$ ) and HT -IMF ( $30.81 \pm 1.67$  vs  $11.7 \pm 1.27$ ) ( $P < 0.05$ )). A  
431 decrease in crypt depth from duodenum to jejunum was also observed in both treatments  
432 (MEM-IMF ( $381 \pm 24.08$   $\mu\text{m}$  vs  $293.46 \pm 13.73$ ) and HT-IMF group ( $366.78 \pm 23.63$  vs  $281.87$   
433  $\pm 7.6$   $\mu\text{m}$ ) ( $P < 0.05$ )). Subsequently, there was a significant increase in villus height: crypt  
434 depth ratio for both IMF treatments in the pig jejunum compared to the duodenum ( $P < 0.05$ ).  
435 There was a significant increase in villus height distally in MEM-IMF fed pigs ( $P < 0.05$ ).  
436 Mucosal thickness was significantly increased in the duodenum ( $816.40 \pm 18.21$   $\mu\text{m}$ ) compared  
437 to the jejunum ( $748.84 \pm 24.63$   $\mu\text{m}$ ) of pigs fed HT-IMF diets ( $P < 0.05$ ). As previously noted  
438 by others (Verdile, Mirmahmoudi, Brevini, & Gandolfi, 2019), it was difficult to observe  
439 Paneth cells in the histology slides of these young pigs. **IL-6 stimulates Paneth cell proliferation**

440 and is critical in maintaining crypt health via Paneth cells and the Wnt signalling pathway  
441 (Andrews, McLean, & Durum, 2018; Jeffery, Goldson, Dainty, Chieppa, & Sobolewski, 2017).

442 Hence, *IL-6* mRNA transcript levels were measured in both the duodenum and jejunum  
443 mucosal scrapings of pigs fed MEM-IMF or HT-IMF diets (Supplementary Figure 5).

444 Interestingly, *IL-6* mRNA transcript levels were significantly increased (3.7 fold) in the  
445 duodenum of pigs fed MEM-IMF diets compared to those fed HT-IMF diets ( $P < 0.01$ ). No

446 differences were detected in *IL-6* mRNA levels in the jejunum ( $P > 0.05$ ).**3.4. Measurement**  
447 **of acidic mucins in mucus layer of pig's small intestine**

448 As there is a higher number of goblet cells in the jejunum of MEM-IMF fed pigs and the  
449 primary function of goblet cells is to secrete mucus, the amount of acidic mucus in the

450 duodenum and jejunum tissue was quantified by Alcian blue dye (Figure 2). In the jejunum  
451 tissue, the amount of acidic mucus was significantly increased in pigs fed MEM-IMF ( $3 \pm 0.24$

452  $\mu\text{g}$  Alcian blue/mg tissue) in comparison with those fed HT-IMF ( $2.48 \pm 0.23 \mu\text{g}$  Alcian  
453 blue/mg tissue) ( $P < 0.05$ ). IMF processing did not influence the amount of acidic mucus in the

454 duodenum tissue. Levels of mucus increased distally with increased amounts of acidic mucus  
455 recorded in the jejunum tissue than the duodenum tissue of pigs for both IMF treatments

456 (MEM-IMF ( $3 \pm 0.24 \mu\text{g}/\text{mg}$  vs  $1.76 \pm 0.18 \mu\text{g}/\text{mg}$ ) and HT-IMF ( $2.48 \pm 0.23 \mu\text{g}/\text{mg}$  vs  $1.75$   
457  $\pm 0.12 \mu\text{g}/\text{mg}$ )  $P < 0.05$ ).

### 458 3.5. Western blot analysis of mucin-2

459 Next, levels of MUC-2 protein, the primary gel-forming mucin in the small intestine, were  
460 quantified by immunoblotting in the small intestinal mucosal scrapings (Figure 3). As MUC-2

461 is a highly glycosylated protein (Arike & Hansson, 2016), two distinct bands were detected at  
462 approximately 200 kDa. In line with Nishida et al. (2009) (Nishida et al., 2009), both bands

463 were included for quantification purposes. Densitometric analysis, employing  $\beta$ -actin as a

464 housekeeping control, showed that protein levels of MUC-2 were significantly higher in the  
465 jejunum of pigs fed MEM-IMF diets compared to those fed HT-IMF diets ( $P < 0.05$ ). However,  
466 protein levels of MUC-2 in the duodenum were similar in both IMF treatment groups. For the  
467 HT-IMF fed pigs, higher levels of MUC-2 were observed in the duodenum compared to the  
468 jejunum ( $P < 0.05$ ).

### 469 **3.6. Effect of IMF processing on biomarkers of gut barrier health and advanced glycation** 470 **endproducts**

471 To further examine the influence of IMF processing on gut barrier health, mRNA transcript  
472 levels of a range of biomarkers were measured in the duodenal and jejunal mucosal scrapings  
473 (Figure 4). In the duodenal mucosal scrapings, the MEM-IMF diet significantly increased  
474 mRNA transcript levels of mucus biomarkers, *mucin-1* (*MUC-1*) ( $P < 0.01$ ), *MUC-2* ( $P <$   
475  $0.001$ ) and tight junction biomarker, *CLDN-1* ( $P < 0.001$ ) compared to the HT-IMF fed pigs  
476 (Figure 4A). IMF processing did not alter mRNA transcript levels of other tight junction  
477 biomarkers (*CLDN-2*, *CLDN-4*, *OCLN*, *ZO-1* and *JAM-A*) in the duodenum ( $P > 0.05$ ). In the  
478 jejunum, mRNA transcript levels of the receptor for advanced glycation end products (*RAGE*),  
479 was significantly decreased in the jejunum (Figure 4B,  $P < 0.05$ ) of pigs fed MEM-IMF diet  
480 compared to those fed HT-IMF diet. No significant differences in mRNA transcript levels were  
481 observed in the jejunum between IMF treatment groups for *MUC-1*, *MUC-2*, *CLDN-1*, *CLDN-*  
482 *2*, *CLDN-4*, *OCLN*, *ZO-1* and *JAM-A* ( $P > 0.05$ ). As an indicator of intestinal inflammation  
483 (Tixier, Lalanne, Just, Galmiche, & Neunlist, 2005), *IL-8* mRNA transcript levels were  
484 measured in the duodenum (Figure 4A) or jejunum (Figure 4B). No significant differences in  
485 *IL-8* mRNA transcript levels were observed in either gut locations with IMF treatment ( $P >$   
486  $0.05$ ).

487 Previously, Bjornvad et al. (2008) linked increased localised *TNF- $\alpha$*  levels to increases in  
488 intestinal permeability (Bjornvad et al., 2008). As such *TNF- $\alpha$*  mRNA transcript levels were  
489 tracked in the duodenum and jejunum mucosal scrapings, revealing no significant difference  
490 in *TNF- $\alpha$*  mRNA expression in either location for pigs fed MEM-IMF compared to those pigs  
491 fed HT-IMF ( $P > 0.05$ ) (Figure 4).

#### 492 **4. Discussion**

493 Feeding MEM-IMF diets to pigs for 28 days resulted in increased goblet cell numbers, mucus  
494 levels, trypsin activity and brush border membrane lactase activity in the upper small intestinal  
495 tract of pigs compared to pigs on HT-IMF diets.

496 The significant increases observed in jejunum goblet cell numbers and acidic mucins was  
497 accompanied with increases in MUC-2 protein levels in pigs fed MEM-IMF. In addition, *MUC-*  
498 *1* and *MUC-2* mRNA transcript levels were significantly increased in the duodenum of these  
499 pigs compared to HT-IMF fed pigs. Goblet cells are scattered, at different densities, throughout  
500 the intestinal tract and function to secrete mucus which lubricates and protects the epithelium  
501 (Kim & Khan, 2013). Newborn infants have inadequate levels of mucus and an underdeveloped  
502 epithelium architecture (Wells, Gao, Groot, Vonk, Ulfman, & Neerven, 2022). Breast milk is  
503 known to promote gut barrier maturity, including increasing mucus production (Dimitroglou  
504 et al., 2022). Evidence is now emerging that reducing thermal processing of IMF or its protein  
505 ingredients can increase mucus secretion and support the intestinal barrier architecture with  
506 some differences based on gut location (Yanqi Li et al., 2018; Y. Li et al., 2013; Navis, Muncan,  
507 et al., 2020; Sun et al., 2022; Wang et al., 2021). Previously, Navis et al. (2020a) observed an  
508 increase in goblet cells, higher alkaline phosphatase and lower lesion scores in the colon of  
509 near-term piglets, fed mildly pasteurised IMF (Navis, Muncan, et al., 2020). A five-day dietary  
510 intervention study was performed with preterm (n = 34 at 106 days gestation) and near-term (n

511 = 18 at 113 days of gestation) piglets (Navis, Muncan, et al., 2020). Piglets received increasing  
512 doses (6 ml/kg/3 h to 10 ml/kg/3 h) of IMF containing 80 g/L of either; (1) mildly pasteurised  
513 whey protein concentrate (WPC) (73°C for 30 s) or (2) extensively heated WPC (73°C for 30  
514 s and 80°C for 6 min) powder by orogastric feeding tube (Navis, Muncan, et al., 2020).  
515 However, this mildly processed IMF did not significantly change mRNA transcript levels of  
516 *MUC-1* and *MUC-2* in the colon or *MUC-2* in the distal small intestine (Navis, Muncan, et al.,  
517 2020). In our study, the colon was not sampled as evidence indicates that WPC is completely  
518 digested in the small intestine with its reported digestible indispensable amino acid score of  
519 107 % at the ileum (Mathai, Liu, & Stein, 2017). The orogastric administration used by Navis  
520 et al. (2020a) may have delayed whey protein digestion resulting in a more distal goblet cell  
521 response (Navis, Muncan, et al., 2020).

522 Although no differences in villus height or crypt depth after our 28 day intervention were  
523 observed, significant increases in duodenal *CLDN-1* mRNA transcript levels was observed in  
524 pigs fed MEM-IMF diets compared to pigs fed HT-IMF diets. A significant increase in CLDN-  
525 1 and a tendency to increase OCLN protein concentration was also observed, previously by us  
526 in an *in vitro* study using polarised Caco-2 monolayers exposed to laboratory scale MEM-IMF  
527 (Bavaro et al., 2021). In other studies, increased CLDN-1 protein levels and *CLDN-1* mRNA  
528 levels have been observed in the jejunum and ileum of pigs where villus height has increased  
529 (Dowley et al., 2021; Ma et al., 2022; Xiao, Jiao, Cao, Song, Hu, & Han, 2016). This CLDN-  
530 1 and villus height association was not observed in our study. In contrast, orogastric  
531 intervention studies with dairy proteins have observed increases in villus height and villus  
532 height:crypt depth ratio in the duodenum, jejunum and ileum (Yanqi Li et al., 2018; Y. Li et  
533 al., 2013; Sun et al., 2022; Wang et al., 2021). Sun et al. (2022) reported significant increases  
534 in intestinal villus height in the proximal, mid and distal small intestine of preterm pigs (n = 56  
535 at 106 days gestation) who received pasteurised liquid IMF by orogastric feeding tube

536 compared to animals who received liquid UHT IMF (Sun et al., 2022). Increasing volumes of  
537 IMF were administered over the 3 days test period (40 ml/kg/day to 120 ml/kg/day). Similarly  
538 Li et al. (2013) treated preterm pigs (n = 55 at 105 days gestation) with IMF powder (24  
539 ml/kg/day to 120 ml/kg/day), by orogastric feeding, for 5 days (Y. Li et al., 2013). Li et al.  
540 (2013) found that villus height in the proximal but not the distal small intestine was  
541 significantly increased in pigs that received IMF with gently processed WPC ( $582 \pm 46 \mu\text{m}$ )  
542 compared with pigs that were fed IMF containing extensively, processed WPC ( $440 \pm 47 \mu\text{m}$ )  
543 (Y. Li et al., 2013). In a follow-up study, administration of WPC alone, resulted in similar  
544 villus height alterations (Yanqi Li et al., 2018). Wang and Zhao (2021) fed unglycated caseinate  
545 (liquid) (with no lactose or heat) and a lactose-glycated caseinate with a high thermal load  
546 ( $100^\circ\text{C}$  for 180 min) to Wistar rats (n = 6) by intra-gastric administration for 7 days (Wang et  
547 al., 2021). Rats fed the unglycated caseinate (400 mg/kg body weight/day) had significantly  
548 higher villus height and villus height:crypt depth ratio in the duodenum, jejunum and ileum  
549 compared with rats fed the glycated caseinate with high thermal load (Wang et al., 2021). In  
550 these acute studies, the test food was the sole source of food administered to the animals for  
551 the duration of the study, albeit additional parenteral nutrition (e.g. carbohydrates, protein, fat,  
552 vitamins, minerals and electrolytes) was supplied. It is worth noting that in our study, IMF was  
553 included in the diet at 35%. This may explain why villus height increases were not observed  
554 with an MEM-IMF dietary intervention. In this study, we did not perform a lactulose: mannitol  
555 test to assess intestinal permeability. However, other markers of increased intestinal  
556 permeability are a reduction in villus height (Y. Li et al., 2014; Y. Li et al., 2013) and increases  
557 in localised TNF- $\alpha$  (Bjornvad et al., 2008). Neither of these responses were observed in our  
558 study, indicating intestinal permeability was unlikely to be affected by IMF processing similar  
559 to that reported by Rasmussen et al. (2016) (Rasmussen et al., 2016). Although Paneth cells  
560 were not observed, mRNA transcript levels of *IL-6*, was significantly increased in the

561 duodenum of pigs fed MEM-IMF compared to HT-IMF fed pigs. This increase may suggest  
562 increased numbers of Paneth cells or a healthy crypt (Andrews et al., 2018)

563 Digestive enzymes were also impacted by IMF diet. There were significant increases in trypsin  
564 activity in the duodenal gut lumen and lactase but lower aminopeptidase N activity in the  
565 duodenal brush border membrane of pigs fed MEM-IMF compared to pigs fed HT-IMF diet.  
566 This significant increase in trypsin activity coincided with increased digestion kinetics of  
567 MEM-IMF (Yihong Chen et al., 2023). Pigs receiving MEM-IMF diet had a significantly  
568 increased protein hydrolysis in the stomach and duodenum compared to pigs fed HT-IMF (599  
569  $\pm 45$  and  $1530 \pm 136$   $\mu\text{mol/g}$  protein vs  $509 \pm 17$  and  $1174 \pm 124$   $\mu\text{mol/g}$  protein) (Yihong  
570 Chen et al., 2023). Although digestion kinetics were not tracked, Wang and Zhao (2021) also  
571 reported significantly increased trypsin and lactase activity in all three small intestinal locations  
572 of rats fed unglycated caseinate (Wang et al., 2021). Lactase activity was also significantly  
573 increased in the proximal and mid small intestine of preterm pigs fed pasteurised liquid IMF in  
574 comparison with UHT processed IMF (Sun et al., 2022). In addition, a significantly higher  
575 lactase activity in the proximal small intestine was observed in piglets fed low heat treated  
576 WPC versus a standard heat treated WPC (Yanqi Li et al., 2018). In our study, significantly  
577 lower levels of aminopeptidase N activity may be correlated with the higher concentrations of  
578 duodenal proline in pigs fed MEM-IMF diet (Yihong Chen et al., 2023). A higher concentration  
579 of free proline suggests that aminopeptidases are able to hydrolyse MEM-IMF peptides more  
580 freely. In contrast, curd formation and protein aggregation of HT-IMF during the gastric phase  
581 of digestion (Y. Chen et al., 2022) may hamper enzyme access in the lumen requiring increased  
582 levels of intestinal brush border aminopeptidase N activity prior to amino acid absorption.  
583 Interestingly, Li et al. (2013) and Navis et al. (2020b) found no effect of processing on  
584 aminopeptidase N, aminopeptidase A and lactase activities in the small intestine (Y. Li et al.,  
585 2013; Navis, Schwebel, et al., 2020). However, digestion kinetics assays were not performed

586 in these studies so whether the different WPCs were digested at different rates could not be  
587 ascertained. Many of these studies have attributed the beneficial gut responses to significantly  
588 lower advanced glycation end products or more specifically, CML levels in the IMFs produced  
589 by lower temperatures (Navis, Schwebel, et al., 2020; Sun et al., 2022). Sun et al. (2022)  
590 reported that administrating IMF liquid with lower levels of advanced glycation end products  
591 results in a lower accumulation of Maillard reaction products in the ileal mucosa of pigs (Sun  
592 et al., 2022). It is widely accepted that high levels of advanced glycation endproducts in the gut  
593 lumen are harmful to the gut barrier (Phuong-Nguyen, McNeill, Aston-Mourney, & Rivera,  
594 2023). Previously, we and others have reported no differences in CML levels in spray dried  
595 IMF powders produced by MEM or HT (Yihong Chen et al., 2021; Yu et al., 2021). However,  
596 a significant decrease in *RAGE* mRNA transcript levels were observed in the jejunum of pigs  
597 fed MEM-IMF diet compared to HT-IMF diet. In the intestine, RAGE serves as a receptor for  
598 CML but also other ligands including other advanced glycation end products (Oshima et al.,  
599 2022). Ligand binding to RAGE activates intestinal inflammatory responses (Body-Malapel et  
600 al., 2019). In our study, mRNA transcript levels of the inflammatory marker *IL-8* were similar  
601 in the duodenum and jejunum of MEM-IMF fed pigs and HT-IMF fed pigs, indicating our IMF  
602 processing was unlikely to result in an inflammatory response via the IL-8 pathway. It has been  
603 observed that more extensive processing of WPC (73°C for 30 s and 80°C for 6 min) will result  
604 in significant increases in colonic IL-8 levels in piglets (Navis, Muncan, et al., 2020). Further  
605 investigations are required to understand better how a decrease in *RAGE* mRNA transcript  
606 levels is physiologically relevant. However, it is also likely that reducing thermal processing  
607 in IMF products has additional benefits apart from reducing advanced glycation end products,  
608 such as preserving whey protein bioactivities (Yanqi Li et al., 2018). Bavaro et al. (2021)  
609 observed that *in vitro* digestion of MEM-IMF released different peptides, with potentially  
610 different bioactivities, than HT-IMF (Bavaro et al., 2021).

611 Unsurprisingly, our study observed physiological and enzymatic differences between different  
612 small intestinal locations in young pigs. Irrespective of treatment type, the number of goblet  
613 cells were significantly higher in the duodenum versus the jejunum. Świąch et al. (2019)  
614 observed a similar trend in young pigs with the duodenum having a higher number of goblet  
615 cells compared to the jejunum (Świąch, Tuśnio, Barszcz, Taciak, & Siwiak, 2019). These  
616 findings disagree with the accepted belief that number of goblet cells increases distally  
617 (Specian & Oliver, 1991). There was also some notable treatment by location interactions.  
618 MEM-IMF fed pigs had increased crypt depth, aminopeptidase A activity and trypsin activity  
619 but decreased villus height in the duodenum compared to the jejunum. HT-IMF fed pigs had  
620 increased crypt depth, mucosa thickness and aminopeptidase A activity but decreased lactase  
621 activity in the duodenum versus the jejunum. In agreement, Li et al. (2018) reported on  
622 increased lactase activity from the proximal to distal small intestine of preterm piglets (Yanqi  
623 Li et al., 2018). However, Sun et al. (2022) observed that brush border lactase activity  
624 decreased along the preterm pig's small intestinal tract (Sun et al., 2022). Regardless of dietary  
625 treatment, reporting on physiological and enzymatic differences between locations in the young  
626 gut is important for nutrition specific recommendations for this life stage.

627 Future work should investigate whether increased mucus production alters bacterial adhesion  
628 in the jejunum. In addition, *in vitro* models of the gut barrier should be employed for  
629 mechanistic studies on mucus production. Ultimately, intervention studies must be performed  
630 in babies to determine if MEM-IMF is easy to digest, promotes gut barrier health and, to  
631 evaluate how it compares to breast milk.

632

## 633 **5. Conclusion**

634 Producing IMF using 1.4 and 0.2  $\mu\text{m}$  filtration membranes has beneficial effects on gut health.  
635 A 35% inclusion of MEM-IMF in the diet of young pigs for 28 days resulted in increased goblet  
636 cell numbers, mucus levels, trypsin activity and lactase activity in the upper small intestine.  
637 This promotion of mucus production in the young gut is superior to IMF produced by high  
638 temperature processing. Next generation IMF should therefore seek to reduce thermal  
639 processing in its quest to mimic breast milk bioactivity.

640

#### 641 **CRedit authorship contribution statement**

642 **Cathal A. Dold:** Conceptualization, Investigation, Methodology, Data curation, Formal  
643 analysis, Resources, Writing – original draft, Writing – review & editing. **Simona L.**

644 **Bavaro:** Conceptualization, Methodology, Resources. **Yihong Chen:** Methodology, Writing  
645 – review & editing. **Michael J. Callanan:** Methodology, Writing – review & editing.

646 **Deirdre Kennedy:** Methodology, Writing – review & editing. **Joe Cassidy:** Methodology,  
647 Writing – review & editing. **Aylin W. Sahin:** Supervision, Writing – review & editing. **John**

648 **Tobin:** Conceptualization, Resources. **Peadar G. Lawlor:** Conceptualization, Methodology,  
649 Resources, Writing – review & editing. **André Brodkorb:** Conceptualization, Resources,

650 Supervision, Writing – review & editing. **Linda Giblin:** Conceptualization, Resources,  
651 Supervision, Writing – review & editing, Project administration, Funding acquisition.

652

#### 653 **Acknowledgements:**

654 This work was funded by Science Foundation Ireland (SFI) and the Department of Agriculture,  
655 Food, and the Marine on behalf of the Government of Ireland under Grant Number (Grant  
656 Number 16/RC/3835 VistaMilk). Cathal Dold is in receipt of a Teagasc Walsh Scholarship.

657

#### 658 **Conflicts of interest statement:**

659 The authors declare that there are no conflicts of interest.

660

## 661 **References**

662 Andrews, C., McLean, M. H., & Durum, S. K. (2018). Cytokine Tuning of Intestinal Epithelial  
663 Function. *Frontiers in immunology*, *9*. <https://doi.org/10.3389/fimmu.2018.01270>.

664 Arike, L., & Hansson, G. C. (2016). The Densely O-Glycosylated MUC2 Mucin Protects the  
665 Intestine and Provides Food for the Commensal Bacteria. *J Mol Biol*, *428*(16), 3221-  
666 3229. <https://doi.org/10.1016/j.jmb.2016.02.010>.

667 Bavaro, S. L., Mamone, G., Picariello, G., Callanan, M. J., Chen, Y., Brodkorb, A., & Giblin,  
668 L. (2021). Thermal or membrane processing for Infant Milk Formula: Effects on protein  
669 digestion and integrity of the intestinal barrier. *Food Chemistry*, *347*, 129019.  
670 <https://doi.org/10.1016/j.foodchem.2021.129019>.

671 Bjornvad, C. R., Thyman, T., Deutz, N. E., Burrin, D. G., Jensen, S. K., Jensen, B. B., . . .  
672 Sangild, P. T. (2008). Enteral feeding induces diet-dependent mucosal dysfunction,  
673 bacterial proliferation, and necrotizing enterocolitis in preterm pigs on parenteral  
674 nutrition. *American Journal of Physiology-Gastrointestinal and Liver Physiology*,  
675 *295*(5), G1092-G1103. <https://doi.org/10.1152/ajpgi.00414.2007>.

676 Body-Malapel, M., Djouina, M., Waxin, C., Langlois, A., Gower-Rousseau, C., Zerbib, P., . . .  
677 Vignal, C. (2019). The RAGE signaling pathway is involved in intestinal  
678 inflammation and represents a promising therapeutic target for Inflammatory Bowel  
679 Diseases. *Mucosal Immunology*, *12*(2), 468-478.  
680 <https://doi.org/https://doi.org/10.1038/s41385-018-0119-z>.

681 Bookhart, L. H., Anstey, E. H., Kramer, M. R., Perrine, C. G., Reis-Reilly, H., Ramakrishnan,  
682 U., & Young, M. F. (2021). A nation-wide study on the common reasons for infant

683 formula supplementation among healthy, term, breastfed infants in US hospitals.  
684 *Matern Child Nutr*, e13294. <https://doi.org/10.1111/mcn.13294>.

685 Bustin, S. A., Benes, V., Garson, J. A., Hellemans, J., Huggett, J., Kubista, M., . . . Wittwer,  
686 C. T. (2009). The MIQE guidelines: minimum information for publication of  
687 quantitative real-time PCR experiments. *Clin Chem*, 55(4), 611-622.  
688 <https://doi.org/10.1373/clinchem.2008.112797>.

689 Chen, Y., Callanan, M., Giblin, L., Tobin, J., & Brodkorb, A. (2022). Comparison of  
690 conventional heat-treated and membrane filtered infant formulas using an in vitro semi-  
691 dynamic digestion method. *Food Funct*. <https://doi.org/10.1039/D2FO00342B>.

692 Chen, Y., Callanan, M., Shanahan, C., Tobin, J., Gamon, L. F., Davies, M. J., . . . Brodkorb,  
693 A. (2021). The Use of Membrane Filtration to Increase Native Whey Proteins in Infant  
694 Formula. *Dairy*, 2(4), 515-529. <https://doi.org/10.3390/dairy2040041>.

695 Chen, Y., Rooney, H., Dold, C., Bavaro, S., Tobin, J., Callanan, M. J., . . . Giblin, L. (2023).  
696 Membrane filtration processing of infant milk formula alters protein digestion in young  
697 pigs. *Food Research International*, 166, 112577.  
698 <https://doi.org/10.1016/j.foodres.2023.112577>.

699 Codex-Alimentarius. (1981). Standards for Infant Formula and Formulas for Special Medical  
700 Purposes Intended for Infants. Codex Stand. 72-1981, FAO/WHO.

701 Commission Regulation. (2005). Commission Regulation (EC) No 2073/2005 of 15 November  
702 2005 on microbiological criteria for foodstuffs. *Official Journal European Commission*  
703 (Vol. L388).

704 Crespo-Piazuelo, D., Gardiner, G. E., Ranjitkar, S., Bouwhuis, M. A., Ham, R., Phelan, J. P., .  
705 . . Lawlor, P. G. (2022). Maternal supplementation with *Bacillus altitudinis* spores  
706 improves porcine offspring growth performance and carcass weight. *British Journal of*  
707 *Nutrition*, 127(3), 403-420. <https://doi.org/10.1017/S0007114521001203>.

708 Dahlqvist, A. (1984). Assay of intestinal disaccharidases. *Scand J Clin Lab Invest*, 44(2), 169-  
709 172. <https://doi.org/10.3109/00365518409161400>.

710 Demers-Mathieu, V. (2022). The immature intestinal epithelial cells in preterm infants play a  
711 role in the necrotizing enterocolitis pathogenesis: A review. *Health Sciences Review*, 4,  
712 100033. <https://doi.org/10.1016/j.hsr.2022.100033>.

713 Dimitroglou, M., Iliodromiti, Z., Christou, E., Volaki, P., Petropoulou, C., Sokou, R., . . .  
714 Iacovidou, N. (2022). Human Breast Milk: The Key Role in the Maturation of Immune,  
715 Gastrointestinal and Central Nervous Systems: A Narrative Review. *Diagnostics*  
716 (*Basel*), 12(9). <https://doi.org/10.3390/diagnostics12092208>.

717 Dowley, A., Sweeney, T., Conway, E., Vigors, S., Yadav, S., Wilson, J., . . . O'Doherty, J. V.  
718 (2021). Effects of Dietary Supplementation with Mushroom or Vitamin D(2)-Enriched  
719 Mushroom Powders on Gastrointestinal Health Parameters in the Weaned Pig. *Animals*  
720 (*Basel*), 11(12). <https://doi.org/10.3390/ani11123603>.

721 Jeffery, V., Goldson, A. J., Dainty, J. R., Chieppa, M., & Sobolewski, A. (2017). IL-6 Signaling  
722 Regulates Small Intestinal Crypt Homeostasis. *J Immunol*, 199(1), 304-311.  
723 <https://doi.org/10.4049/jimmunol.1600960>.

724 Kim, J. J., & Khan, W. I. (2013). Goblet cells and mucins: role in innate defense in enteric  
725 infections. *Pathogens*, 2(1), 55-70. <https://doi.org/10.3390/pathogens2010055>.

726 Li, Y., Jensen, M. L., Chatterton, D. E., Jensen, B. B., Thymann, T., Kvistgaard, A. S., &  
727 Sangild, P. T. (2014). Raw bovine milk improves gut responses to feeding relative to  
728 infant formula in preterm piglets. *Am J Physiol Gastrointest Liver Physiol*, 306(1), G81-  
729 90. <https://doi.org/10.1152/ajpgi.00255.2013>.

730 Li, Y., Nguyen, D. N., Obelitz-Ryom, K., Andersen, A., Thymann, T., Chatterton, D. E. W., .  
731 . . Sangild, P. T. (2018). Bioactive Whey Protein Concentrate and Lactose Stimulate

732 Gut Function in Formula-fed Preterm Pigs. *Journal of pediatric gastroenterology and*  
733 *nutrition*, 66, 12X 134. <https://doi.org/10.1097/MPG.0000000000001699>.

734 Li, Y., Østergaard, M. V., Jiang, P., Chatterton, D. E., Thymann, T., Kvistgaard, A. S., &  
735 Sangild, P. T. (2013). Whey protein processing influences formula-induced gut  
736 maturation in preterm pigs. *J Nutr*, 143(12), 1934-1942.  
737 <https://doi.org/10.3945/jn.113.182931>.

738 Livak, K. J., & Schmittgen, T. D. (2001). Analysis of relative gene expression data using real-  
739 time quantitative PCR and the 2(-Delta Delta C(T)) Method. *Methods*, 25(4), 402-408.  
740 <https://doi.org/10.1006/meth.2001.1262>.

741 Lund, P., Bechshøft, M. R., Ray, C. A., & Lund, M. N. (2021). Effect of Processing of Whey  
742 Protein Ingredient on Maillard Reactions and Protein Structural Changes in Powdered  
743 Infant Formula. *Journal of Agricultural and Food Chemistry*.  
744 <https://doi.org/10.1021/acs.jafc.1c05612>.

745 Ma, X., Hao, Y., Mao, R., Yang, N., Zheng, X., Li, B., . . . Wang, J. (2022). Effects of dietary  
746 supplementation of bovine lactoferrin on growth performance, immune function and  
747 intestinal health in weaning piglets. *BioMetals*. [https://doi.org/10.1007/s10534-022-](https://doi.org/10.1007/s10534-022-00461-x)  
748 [00461-x](https://doi.org/10.1007/s10534-022-00461-x).

749 Mamone, G., & Picariello, G. (2023). Optimized extraction and large-scale proteomics of pig  
750 jejunum brush border membranes for use in in vitro digestion models. *Food Res Int*,  
751 164, 112326. <https://doi.org/10.1016/j.foodres.2022.112326>.

752 Mathai, J. K., Liu, Y., & Stein, H. H. (2017). Values for digestible indispensable amino acid  
753 scores (DIAAS) for some dairy and plant proteins may better describe protein quality  
754 than values calculated using the concept for protein digestibility-corrected amino acid  
755 scores (PDCAAS). *British Journal of Nutrition*, 117(4), 490-499.  
756 <https://doi.org/10.1017/S0007114517000125>.

757 National Research Council. (2012). *Nutrient Requirements of Swine: Eleventh Revised Edition*.  
758 Washington, DC: The National Academies Press.

759 Navis, M., Muncan, V., Sangild, P. T., Møller Willumsen, L., Koelink, P. J., Wildenberg, M.  
760 E., . . . Renes, I. B. (2020). Beneficial Effect of Mildly Pasteurized Whey Protein on  
761 Intestinal Integrity and Innate Defense in Preterm and Near-Term Piglets. *Nutrients*,  
762 *12*(4). <https://doi.org/10.3390/nu12041125>.

763 Navis, M., Schwebel, L., Soendergaard Kappel, S., Muncan, V., Sangild, P. T., Abrahamse, E.,  
764 . . . Renes, I. B. (2020). Mildly Pasteurized Whey Protein Promotes Gut Tolerance in  
765 Immature Piglets Compared with Extensively Heated Whey Protein. *Nutrients*, *12*(11),  
766 3391. <https://doi.org/10.3390/nu12113391>.

767 Neu, J. (2007). Gastrointestinal maturation and implications for infant feeding. *Early Hum Dev*,  
768 *83*(12), 767-775. <https://doi.org/10.1016/j.earlhumdev.2007.09.009>.

769 Nishida, K., Kamizato, M., Kawai, T., Masuda, K., Takeo, K., Teshima-Kondo, S., . . .  
770 Rokutan, K. (2009). Interleukin-18 is a crucial determinant of vulnerability of the  
771 mouse rectum to psychosocial stress. *Faseb j*, *23*(6), 1797-1805.  
772 <https://doi.org/10.1096/fj.08-125005>.

773 Oshima, Y., Harashima, A., Munesue, S., Kimura, K., Leerach, N., Goto, H., . . . Yamamoto,  
774 Y. (2022). Dual Nature of RAGE in Host Reaction and Nurturing the Mother-Infant  
775 Bond. *Int J Mol Sci*, *23*(4). <https://doi.org/10.3390/ijms23042086>.

776 Phosanam, A., Chandrapala, J., Huppertz, T., Adhikari, B., & Zisu, B. (2021). In vitro digestion  
777 of infant formula model systems: Influence of casein to whey protein ratio.  
778 *International Dairy Journal*, *117*, 105008.  
779 <https://doi.org/10.1016/j.idairyj.2021.105008>.

780 Phuong-Nguyen, K., McNeill, B. A., Aston-Mourney, K., & Rivera, L. R. (2023). Advanced  
781 Glycation End-Products and Their Effects on Gut Health. *Nutrients*, 15(2), 405.  
782 <https://doi.org/10.3390/nu15020405>.

783 Rasmussen, S. O., Martin, L., Østergaard, M. V., Rudloff, S., Li, Y., Roggenbuck, M., . . .  
784 Sangild, P. T. (2016). Bovine colostrum improves neonatal growth, digestive function,  
785 and gut immunity relative to donor human milk and infant formula in preterm pigs. *Am*  
786 *J Physiol Gastrointest Liver Physiol*, 311(3), G480-491.  
787 <https://doi.org/10.1152/ajpgi.00139.2016>.

788 Renz, H., Brandtzaeg, P., & Hornef, M. (2011). The impact of perinatal immune development  
789 on mucosal homeostasis and chronic inflammation. *Nat Rev Immunol*, 12(1), 9-23.  
790 <https://doi.org/10.1038/nri3112>.

791 Smirnov, A., Sklan, D., & Uni, Z. (2004). Mucin Dynamics in the Chick Small Intestine Are  
792 Altered by Starvation. *The Journal of Nutrition*, 134(4), 736-742.  
793 <https://doi.org/10.1093/jn/134.4.736>.

794 Specian, R. D., & Oliver, M. G. (1991). Functional biology of intestinal goblet cells. *American*  
795 *Journal of Physiology-Cell Physiology*, 260(2), C183-C193.  
796 <https://doi.org/10.1152/ajpcell.1991.260.2.C183>.

797 Sun, J., Akıllıoğlu, H. G., Aasmul-Olsen, K., Ye, Y., Lund, P., Zhao, X., . . . Bering, S. B.  
798 (2022). Ultra-high Temperature Treatment and Storage of Infant Formula Induces  
799 Dietary Protein Modifications, gut Dysfunction and Inflammation in Preterm Pigs. *Mol*  
800 *Nutr Food Res*, e2200132. <https://doi.org/10.1002/mnfr.202200132>.

801 Świąch, E., Tuśnio, A., Barszcz, M., Taciak, M., & Siwiak, E. (2019). Goblet cells and mucus  
802 layer in the gut of young pigs: Response to dietary contents of threonine and non-  
803 essential amino acids. *J Anim Physiol Anim Nutr (Berl)*, 103(3), 894-905.  
804 <https://doi.org/10.1111/jpn.13086>.

805 Tixier, E., Lalanne, F., Just, I., Galmiche, J.-P., & Neunlist, M. (2005). Human  
806 mucosa/submucosa interactions during intestinal inflammation: involvement of the  
807 enteric nervous system in interleukin-8 secretion. *Cellular Microbiology*, 7(12), 1798-  
808 1810. <https://doi.org/https://doi.org/10.1111/j.1462-5822.2005.00596.x>.

809 Verdile, N., Mirmahmoudi, R., Brevini, T. A. L., & Gandolfi, F. (2019). Evolution of pig  
810 intestinal stem cells from birth to weaning. *Animal*, 13(12), 2830-2839.  
811 <https://doi.org/https://doi.org/10.1017/S1751731119001319>.

812 Wada, Y., & Lönnerdal, B. (2015). Effects of Industrial Heating Processes of Milk-Based  
813 Enteral Formulas on Site-Specific Protein Modifications and Their Relationship to in  
814 Vitro and in Vivo Protein Digestibility. *J Agric Food Chem*, 63(30), 6787-6798.  
815 <https://doi.org/10.1021/acs.jafc.5b02189>.

816 Wang, X. P., & Zhao, X. H. (2021). Lactose Glycation of the Maillard-Type Impairs the  
817 Benefits of Caseinate Digest to the Weaned Rats for Intestinal Morphology and Serum  
818 Biochemistry. *Foods*, 10(9). <https://doi.org/10.3390/foods10092104>.

819 Wells, J. M., Gao, Y., Groot, N. d., Vonk, M. M., Ulfman, L., & Neerven, R. J. J. v. (2022).  
820 Babies, Bugs, and Barriers: Dietary Modulation of Intestinal Barrier Function in Early  
821 Life. *Annual Review of Nutrition*, 42(1), 165-200. <https://doi.org/10.1146/annurev-nutr-122221-103916>.

823 Xiao, K., Jiao, L., Cao, S., Song, Z., Hu, C., & Han, X. (2016). Whey protein concentrate  
824 enhances intestinal integrity and influences transforming growth factor- $\beta$ 1 and  
825 mitogen-activated protein kinase signalling pathways in piglets after  
826 lipopolysaccharide challenge. *British Journal of Nutrition*, 115(6), 984-993.  
827 <https://doi.org/10.1017/S0007114515005085>.

828 Ye, Y., Engholm-Keller, K., Fang, Y., Nielsen, C. F., Jordà, A., Lund, M. N., & Chatterton, D.  
829 E. W. (2021). UHT treatment and storage of liquid infant formula affects protein

830 digestion and release of bioactive peptides. *Food Funct.*  
831 <https://doi.org/10.1039/d1fo02619d>.  
832 Yu, X., Leconte, N., Méjean, S., Garric, G., Even, S., Henry, G., . . . Deglaire, A. (2021). Semi-  
833 industrial production of a minimally processed infant formula powder using membrane  
834 filtration. *Journal of Dairy Science*. [https://doi.org/https://doi.org/10.3168/jds.2020-](https://doi.org/https://doi.org/10.3168/jds.2020-19529)  
835 [19529](https://doi.org/https://doi.org/10.3168/jds.2020-19529).  
836

837 **Figure Legends**

838 **Figure 1.** Influence of MEM-IMF (white) or HT-IMF (black) diets on trypsin activity  
839 (mU/mg total protein) in gut lumen collected from pigs. Values are reported as means  $\pm$  SEM  
840 (n = 9 pigs per treatment). Different uppercase letters within the same intestinal location  
841 indicates significant differences between treatment types ( $P < 0.05$ ). Different lowercase  
842 letters within the same treatment type indicates a significant difference between intestinal  
843 locations ( $P < 0.05$ ). MEM-IMF = membrane filtered infant milk formula; HT-IMF = high-  
844 temperature infant milk formula.

845

846 **Figure 2.** Measurement of acidic mucins by Alcian blue dye ( $\mu\text{g}$  Alcian blue/mg tissue) in  
847 the tissue of pigs fed MEM-IMF (grey dots) or HT-IMF (black dots) diets for 28 days.  
848 Samples from the pig duodenum and jejunum were collected at slaughter 3 h after final  
849 feeding. Values are reported as means  $\pm$  SEM (n = 10 pigs per treatment). Different  
850 uppercase letters within the same intestinal location indicates significant differences between  
851 IMF dietary treatment types ( $P < 0.05$ ). Different lowercase letters within the same IMF  
852 dietary treatment types indicates significant differences between intestinal locations ( $P <$   
853  $0.05$ ). MEM-IMF = membrane filtered infant milk formula; HT-IMF = high-temperature  
854 infant milk formula.

855

856 **Figure 3.** Western blot analysis of mucin-2 (MUC-2) in the mucosal scrapings of pigs fed  
857 MEM-IMF (white) or HT-IMF (black) diets for 28 days. Mucosal scrapings were collected at  
858 slaughter 3 h after final feeding. (A) Immunoreactive bands were quantified using Image Lab  
859 6.1 software. (B) Quantification of MUC-2 bands were calibrated against the intensity of the  
860 housekeeping  $\beta$ -actin band. Values are reported as means  $\pm$  SEM (n = 3 pigs per treatment).  
861 Different uppercase letters within the same intestinal location indicates significant differences

862 between IMF dietary treatment types ( $P < 0.05$ ). Different lowercase letters within the same  
863 IMF dietary treatment types indicates significant differences between intestinal locations ( $P <$   
864  $0.05$ ). MEM-IMF = membrane filtered infant milk formula; HT-IMF = high-temperature  
865 infant milk formula.

866

867 **Figure 4.** mRNA transcript levels in (A) duodenum and (B) jejunum mucosal scrapings of  
868 pigs fed MEM-IMF (white) or HT-IMF (black) diets for 28 days. Mucosal scrapings were  
869 collected at slaughter 3 h after final feeding. Values are reported as means  $\pm$  SEM (n = 8 pigs  
870 per treatment). The relative quantification of target mRNA was calculated using the reference  
871 gene RPLP0 following the  $2^{-\Delta\Delta C_t}$  method. Transcript levels are expressed as the fold change  
872 relative to the mean value of the HT-IMF (control) diet. Significant differences between diets  
873 for each individual gene are indicated by \*  $P < 0.05$ , \*\*  $P < 0.01$  and \*\*\*  $P < 0.001$ . *MUC-1*,  
874 *mucin-1*; *MUC-2*, *mucin-2*; *CLDN-1*, *claudin-1*; *CLDN-2*, *claudin-2*; *CLDN-4*, *claudin-4*;  
875 *OCN*, *occludin*; *ZO-1*, *zona occludens-1*; *JAM-A*, *junctional adhesion molecule A*; *RAGE*,  
876 *receptor for advanced glycation end products*; *IL-8*, *interleukin 8*; *TNF- $\alpha$* , *tumor necrosis*  
877 *factor alpha*. MEM-IMF = membrane filtered infant milk formula; HT-IMF = high-  
878 temperature infant milk formula.

879

880

881 **Table 1.** Brush border membrane enzymatic activity in pigs fed MEM-IMF or HT-IMF diets  
882 for 28 days. Enzymatic activities were measured in isolated brush border membrane vesicles  
883 (n = 7 pigs per treatment) 3 h after final feeding. Values are reported as means  $\pm$  SEM. Different  
884 uppercase letters within the same intestinal location indicates significant differences between  
885 IMF dietary treatment types ( $P < 0.05$ ). Different lowercase letters within the same IMF dietary  
886 treatment types indicates significant differences between intestinal locations ( $P < 0.05$ ). MEM-  
887 IMF = membrane filtered infant milk formula; HT-IMF = high-temperature infant milk  
888 formula.

	MEM-IMF	HT-IMF
<b>Duodenum brush border membrane</b>		
Aminopeptidase N (U/mg cellular protein)	5.23 $\pm$ 0.26 <sup>Ba</sup>	7.44 $\pm$ 0.69 <sup>Aa</sup>
Aminopeptidase A (mU/mg cellular protein)	176.52 $\pm$ 13.83 <sup>Aa</sup>	155.17 $\pm$ 22.83 <sup>Aa</sup>
Intestinal Alkaline Phosphatase (U/mg cellular protein)	185.53 $\pm$ 29.68 <sup>Aa</sup>	167.44 $\pm$ 30.49 <sup>Aa</sup>
Lactase (nmol glucose/mg cellular protein)	166.59 $\pm$ 22.09 <sup>Aa</sup>	110.75 $\pm$ 7.21 <sup>Bb</sup>
<b>Jejunum brush border membrane</b>		
Aminopeptidase N (U/mg cellular protein)	6.59 $\pm$ 0.47 <sup>Ab</sup>	6.95 $\pm$ 1.13 <sup>Aa</sup>
Aminopeptidase A (mU/mg cellular protein)	29.82 $\pm$ 3.46 <sup>Ab</sup>	57.44 $\pm$ 18.17 <sup>Ab</sup>
Intestinal Alkaline Phosphatase (U/mg cellular protein)	135.07 $\pm$ 10.82 <sup>Aa</sup>	154.27 $\pm$ 27.13 <sup>Aa</sup>
Lactase (nmol glucose/mg cellular protein)	154.16 $\pm$ 10.30 <sup>Aa</sup>	168.45 $\pm$ 18.04 <sup>Aa</sup>

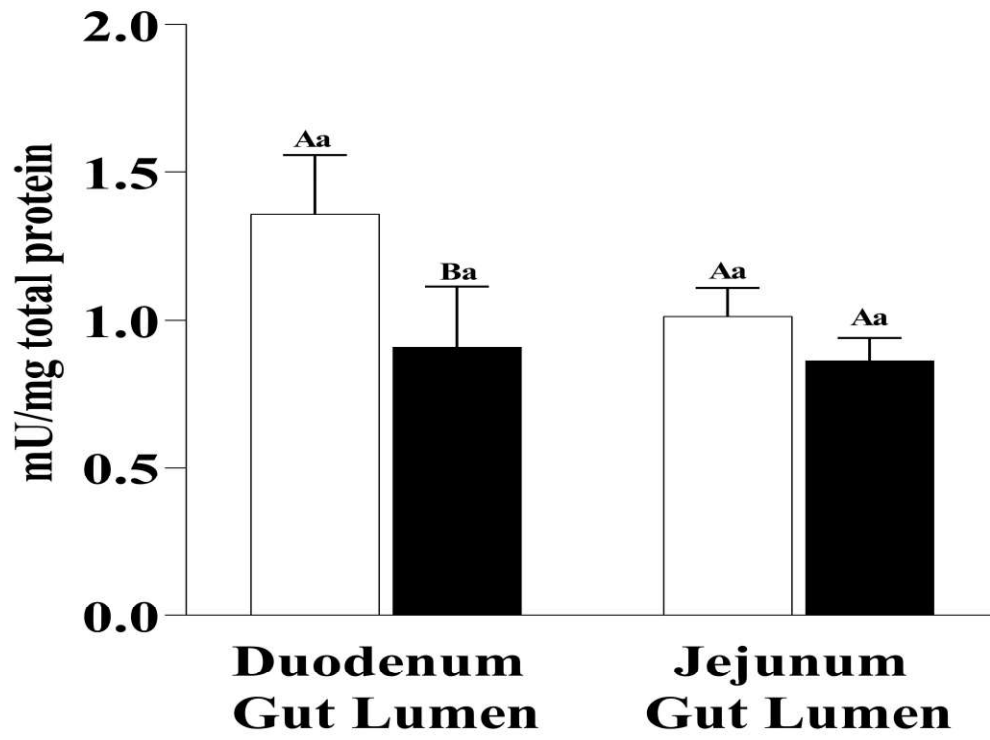
889

890 **Table 2.** Histological analysis of duodenum and jejunum of pigs fed MEM-IMF or HT-IMF  
891 diets for 28 days. Values are reported as means  $\pm$  SEM (MEM-IMF, n = 8 pigs, HT-IMF, n =  
892 6 pigs). Different uppercase letters within the same intestinal location indicates significant  
893 differences between IMF dietary treatment ( $P < 0.05$ ). Different lowercase letters within the  
894 same IMF dietary treatment indicates significant differences between intestinal locations ( $P <$   
895  $0.05$ ). MEM-IMF = membrane filtered infant milk formula; HT-IMF = high-temperature infant  
896 milk formula.

	MEM-IMF	HT-IMF
<b>Number of goblet cells</b>		
Duodenum	27.98 $\pm$ 3.56 <sup>Aa</sup>	30.81 $\pm$ 1.67 <sup>Aa</sup>
Jejunum	17.39 $\pm$ 1.43 <sup>Ab</sup>	11.7 $\pm$ 1.27 <sup>Bb</sup>
<b>Mucosa thickness (<math>\mu\text{m}</math>)</b>		
Duodenum	785.68 $\pm$ 29.38 <sup>Aa</sup>	816.40 $\pm$ 18.21 <sup>Aa</sup>
Jejunum	770.51 $\pm$ 31.85 <sup>Aa</sup>	748.84 $\pm$ 24.63 <sup>Ab</sup>
<b>Villus height (<math>\mu\text{m}</math>)</b>		
Duodenum	404.66 $\pm$ 22.34 <sup>Ab</sup>	449.60 $\pm$ 24.72 <sup>Aa</sup>
Jejunum	477.06 $\pm$ 29.54 <sup>Aa</sup>	466.96 $\pm$ 26.19 <sup>Aa</sup>
<b>Crypt depth (<math>\mu\text{m}</math>)</b>		
Duodenum	381 $\pm$ 24.08 <sup>Aa</sup>	366.78 $\pm$ 23.63 <sup>Aa</sup>
Jejunum	293.46 $\pm$ 13.73 <sup>Ab</sup>	281.87 $\pm$ 7.6 <sup>Ab</sup>
<b>Villus height: crypt depth ratio</b>		
Duodenum	1.19 $\pm$ 0.11 <sup>Ab</sup>	1.33 $\pm$ 0.15 <sup>Ab</sup>
Jejunum	1.75 $\pm$ 0.14 <sup>Aa</sup>	1.74 $\pm$ 0.12 <sup>Aa</sup>

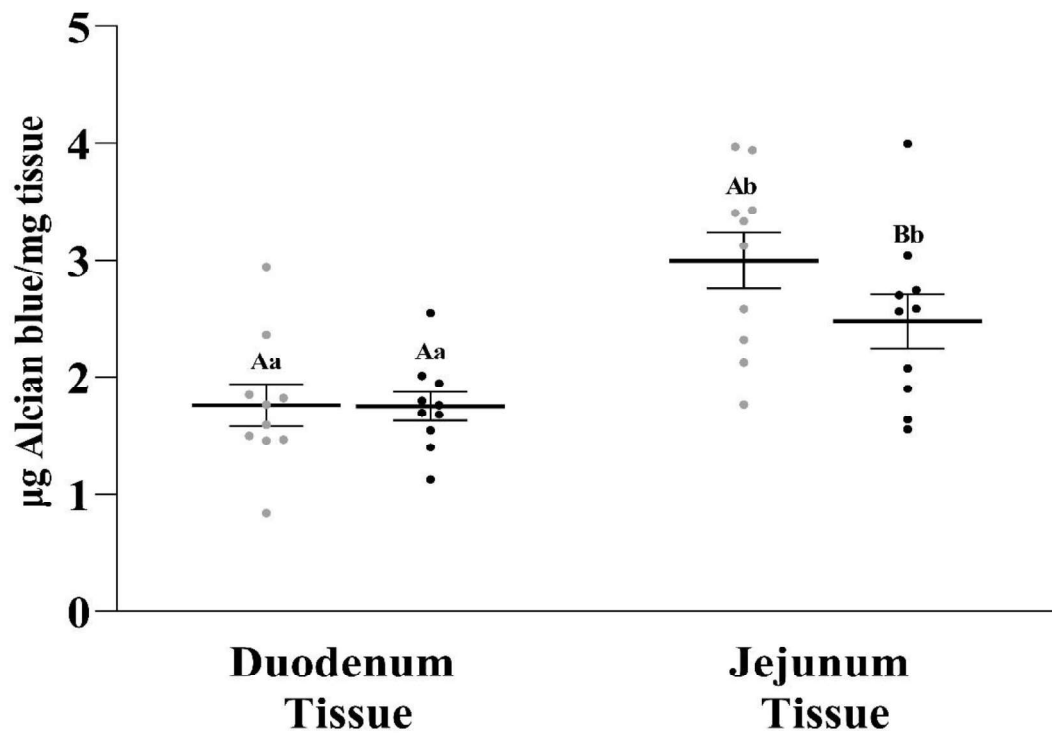
897

898 **Figure 1.**



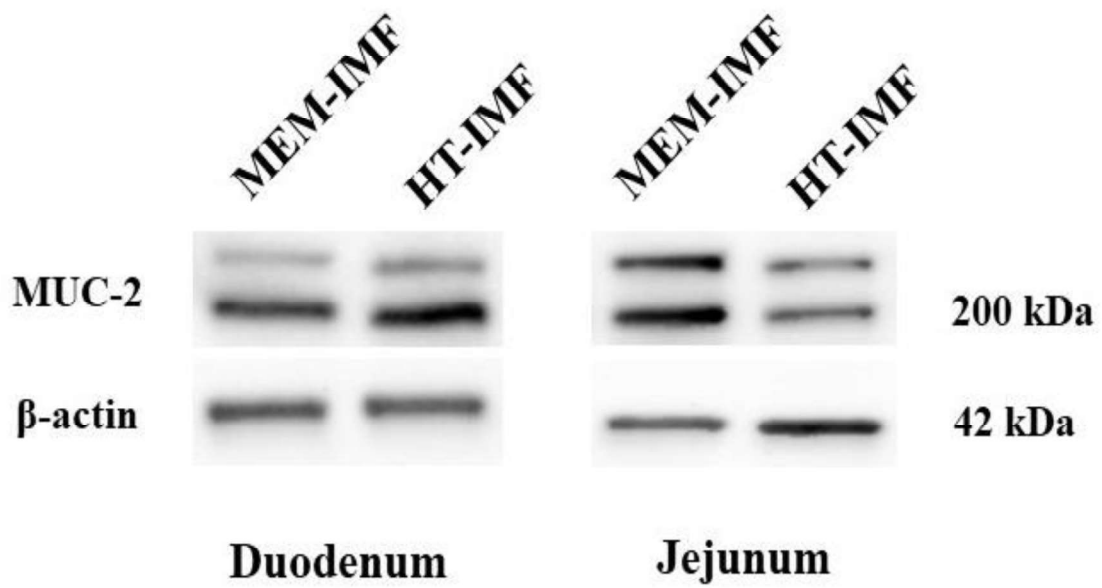
899  
900

901 **Figure 2.**

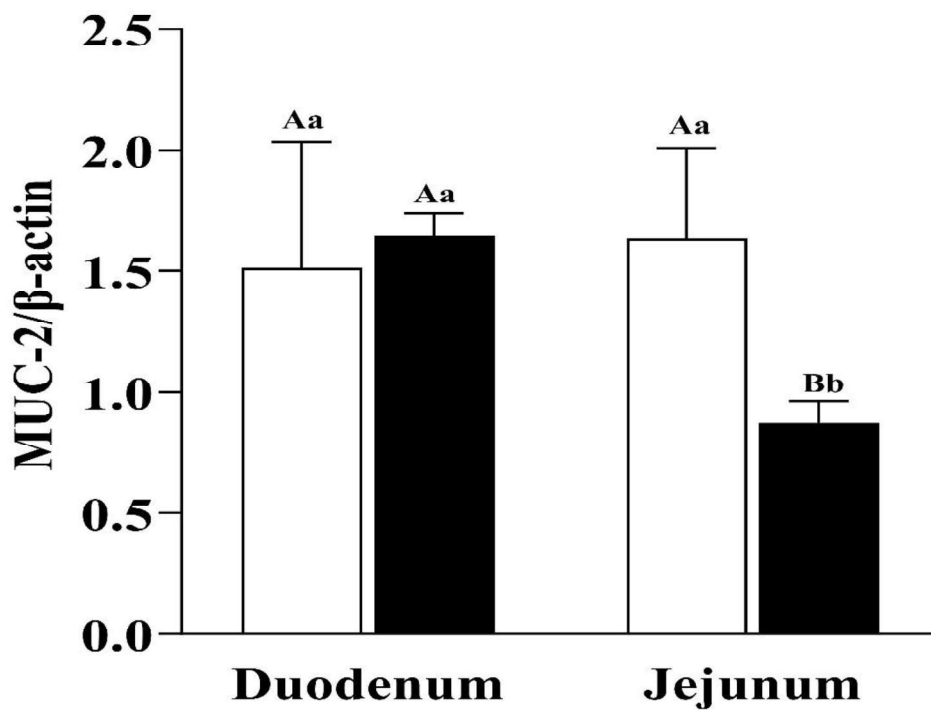


902  
903

904 **Figure 3.**  
905 **A)**

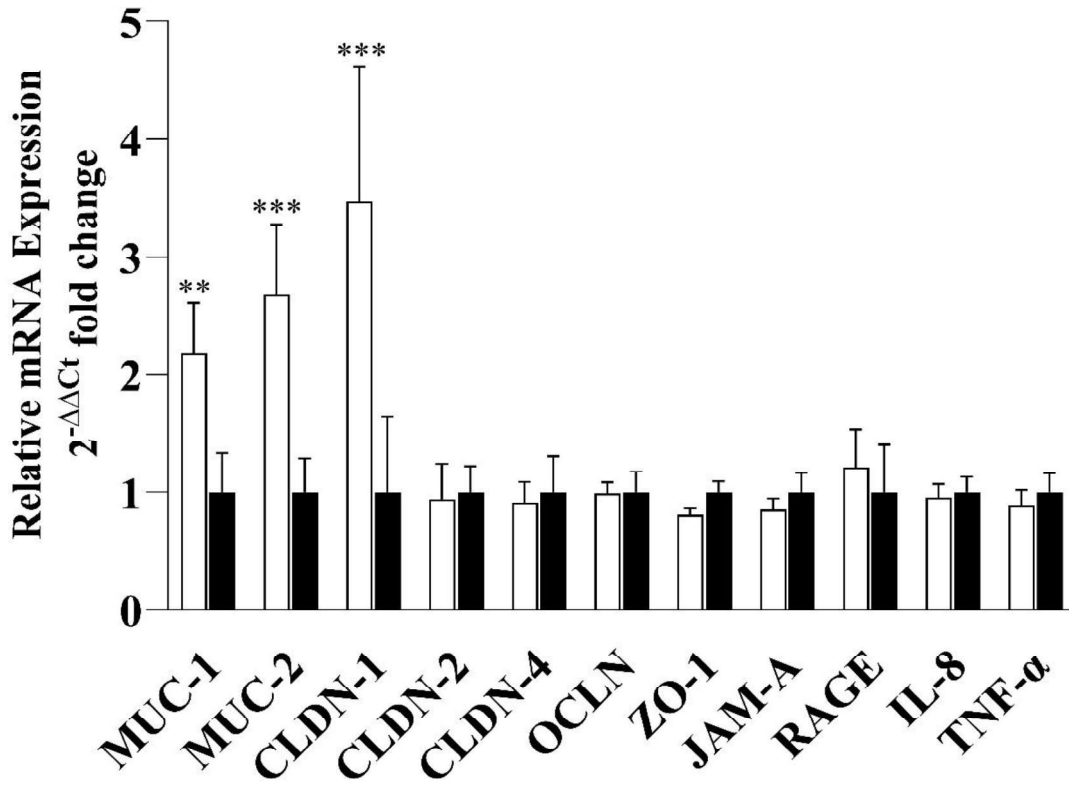


906 **B)**  
907

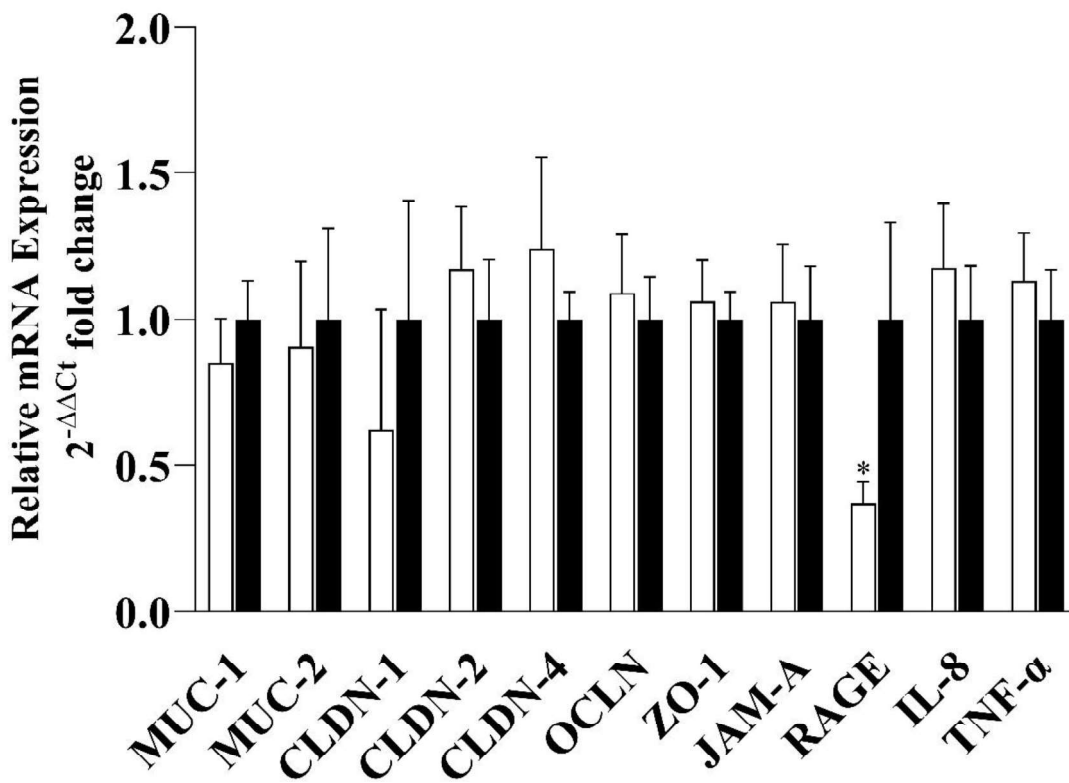


908  
909  
910

911 **Figure 4.**  
 912 **A)**



913 **B)**  
 914



915  
 916

917 **Supplementary Material**

918

919 **Supplementary Table 1.** Gene name, GenBank accession number, primer sequences,

920 annealing temperature and amplicon size for RT-qPCR analysis.

Gene	GenBank Accession Number	Primer sequences (5'-3')	T <sub>a</sub> (°C)	Amplicon size (bp)
<i>RPLP0</i>	NM_001098598.1	F: GACAAAGTGGGAGCCAGTGA R: CAGGGTTGTAGATGCTGCCA	56	112
<i>MUC-1</i>	XM_021089729.1	F: AGTCCATGTTGGCACCTCC R: GGAGTACCTTTGCTGACTGG	55	117
<i>MUC-2</i>	XM_013989745.1	F: TCTGGATCCGCAGCTCTCTGG R: CACTGGGCTGGGAGACAGGT	60	157
<i>CLDN-1</i>	NM_001244539.1	F: ACCGTGTGGGAACAACCAGA R: ACACATGAAAATGGCTTCCCTCC	62	195
<i>CLDN-2</i>	NM_001161638.1	F: GCATCATTTCCTCCCTGTT R: TCTTGGCTTTGGGTGGTT	60	156
<i>CLDN-4</i>	NM_001161637.1	F: CAACTGCGTGGATGATGAGA R: CCAGGGGATTGTAGAAGTCG	60	140
<i>OCN</i>	NM_001163647.2	F: TCCTGGGTGTGATGGTGTTTC R: CGTAGAGTCCAGTCACCGCA	63	144
<i>ZO-1</i>	XM_003353439.2	F: ATGGCGGAAAGTGAACCTCG R: TCACACCCTGCTTAGAATCCG	55	199
<i>JAM-A</i>	NM_001128444.1	F: CCAGGAAAGACACAGGGACG R: GGTTCCCGATGGTAGCAGAG	58	144
<i>RAGE</i>	NM_001123218.1	F: AGGTGGAGCTGTACCTCCTG R: TCCTTGGTCCAGTGGATTTG	60	87
<i>IL-6</i>	NM_214399.1	F: TGGCTACTGCCTTCCCTACC R: CAGAGATTTTGCCGAGGATG	60	132
<i>IL-8</i>	NM_213867.1	F: GAAGAGAAGTGAAGCAACAACA R: TTGTGTTGGCATCTTTACTGAGA	60	99
<i>TNF-α</i>	NM_214022.1	F: CACGTTGTAGCCAATGTCAAAG R: GAGGTACAGCCCATCTGTCG	60	129

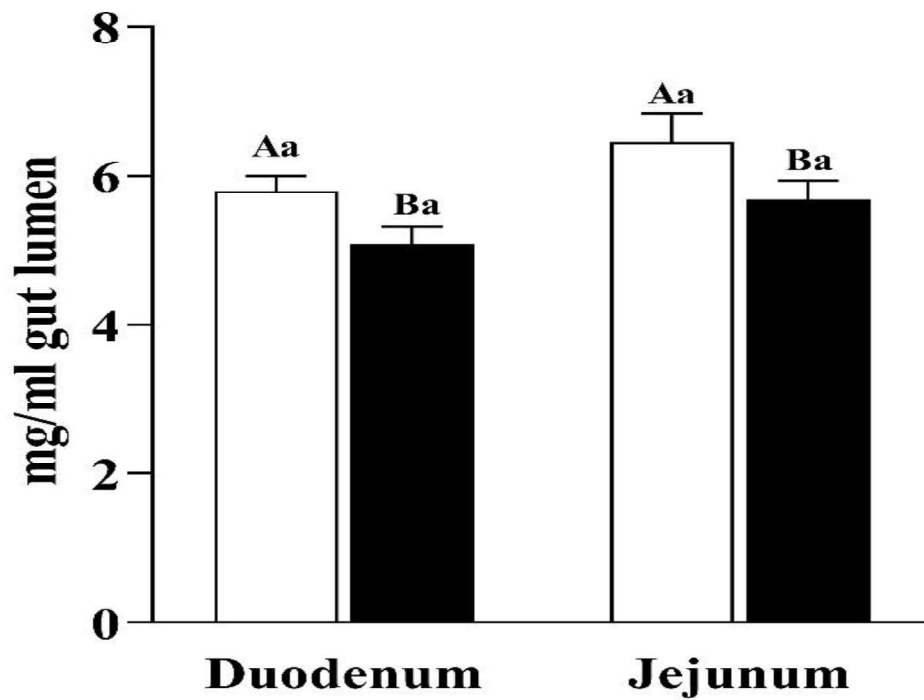
921 T<sub>a</sub>, annealing temperature; bp, base pairs; *RPLP0*, ribosomal protein lateral stalk subunit P0;

922 *MUC-1*, mucin-1; *MUC-2*, mucin-2; *CLDN-1*, claudin-1; *CLDN-2*, claudin-2; *CLDN-4*,

923 *claudin-4*; *OCN*, occludin; *ZO-1*, zona occludens-1; *JAM-A*, junctional adhesion molecule

924 *A*; *RAGE*, receptor for advanced glycation end products. *IL-6*, interleukin 6; *IL-8*, interleukin

925 *8*; *TNF-α*, tumor necrosis factor alpha.



926

927

928

929

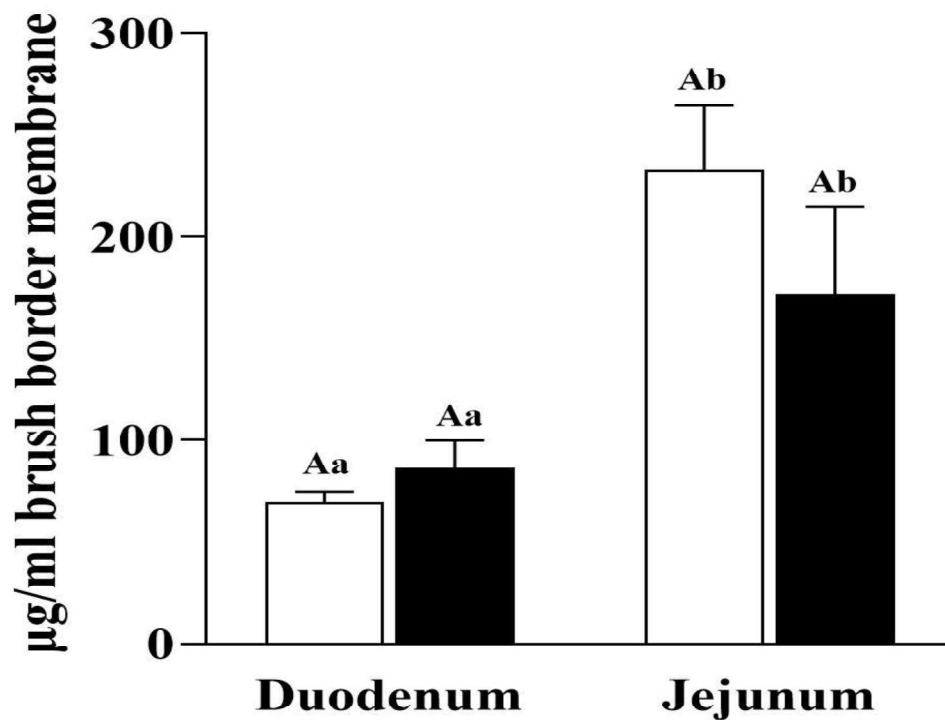
930

931

932

933

**Supplementary Figure 1.** Total protein concentration (mg/ml gut lumen) in gut lumen collected from the pigs following slaughter. MEM-IMF, membrane filtered infant milk formula (white); HT-IMF, high-temperature infant milk formula (black). Values are reported as means  $\pm$  SEM (n = 9). Different uppercase letters within the same intestinal location indicates significant differences between treatment types ( $P < 0.05$ ). Different lowercase letters within the same treatment type indicates significant differences between intestinal locations ( $P < 0.05$ ).

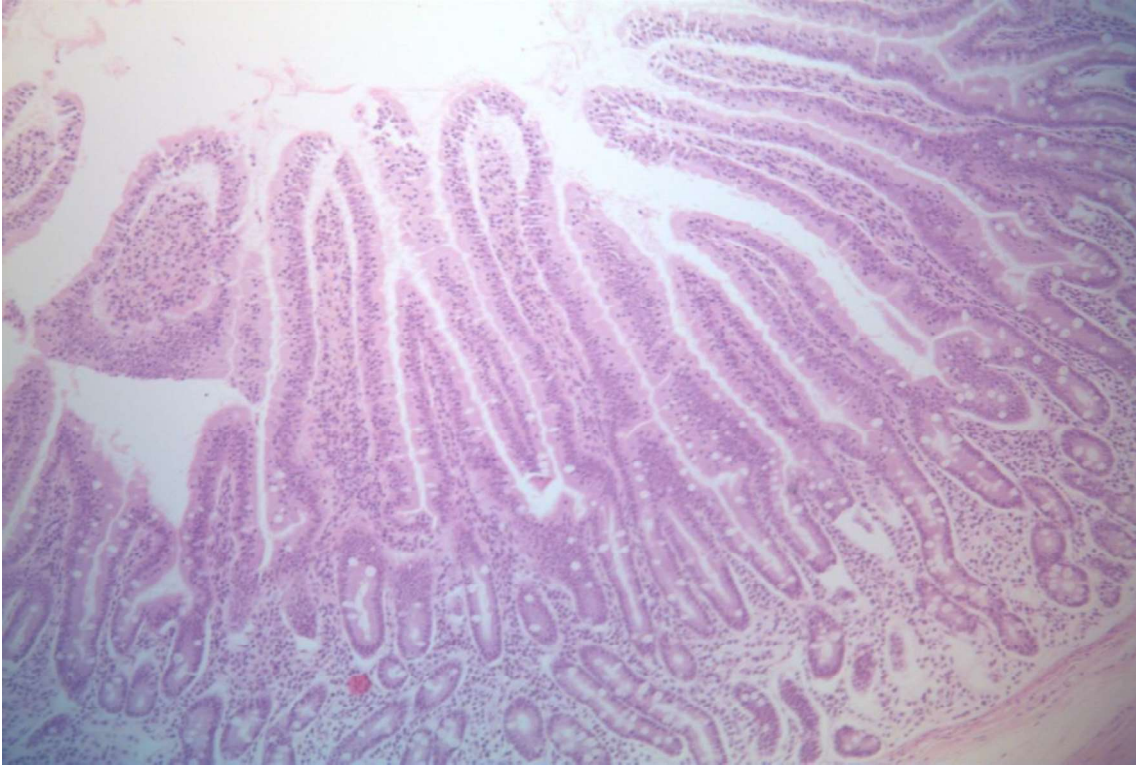


934

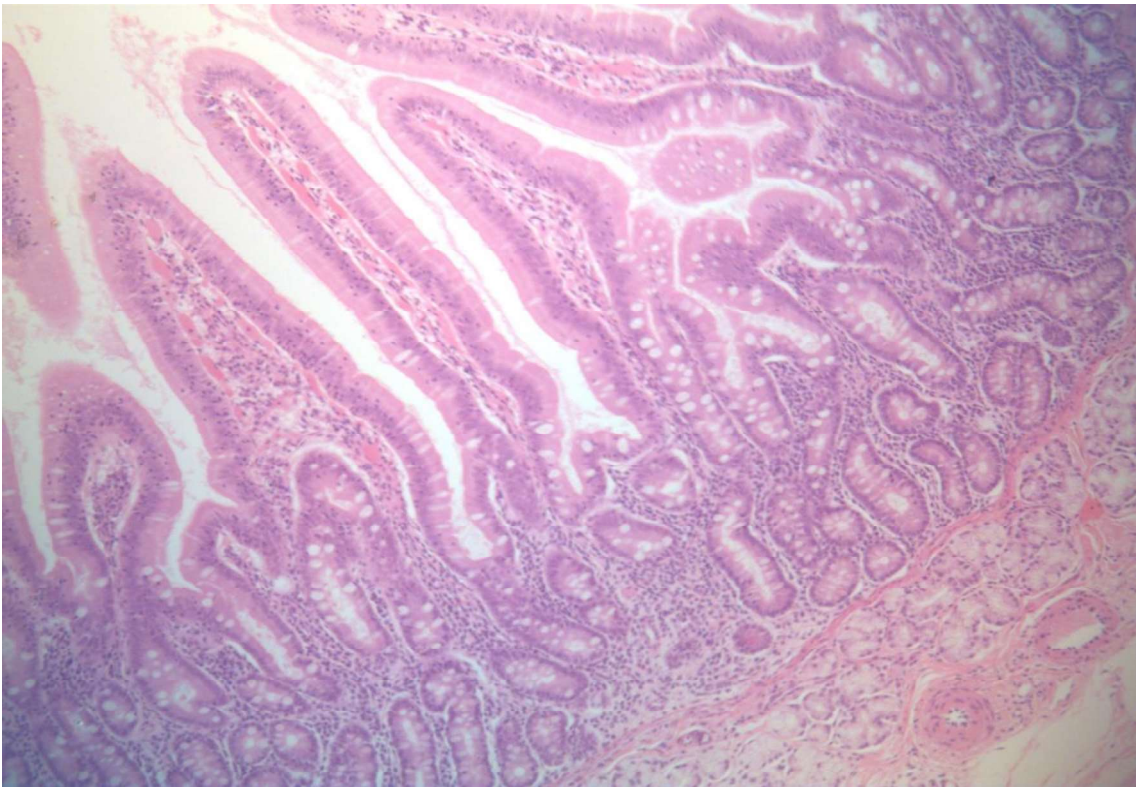
935 **Supplementary Figure 2.** Cellular protein concentration ( $\mu\text{g/ml}$  brush border membrane) in  
 936 brush border membrane vesicles isolated from the pigs small intestinal mucosal scrapings.  
 937 MEM-IMF, membrane filtered infant milk formula (white); HT-IMF, high-temperature infant  
 938 milk formula (black). Values are reported as means  $\pm$  SEM ( $n = 7$ ). Different uppercase  
 939 letters within the same intestinal location indicates significant differences between treatment  
 940 types ( $P < 0.05$ ). Different lowercase letters within the same treatment type indicates  
 941 significant differences between intestinal locations ( $P < 0.05$ ).

942

943 A)



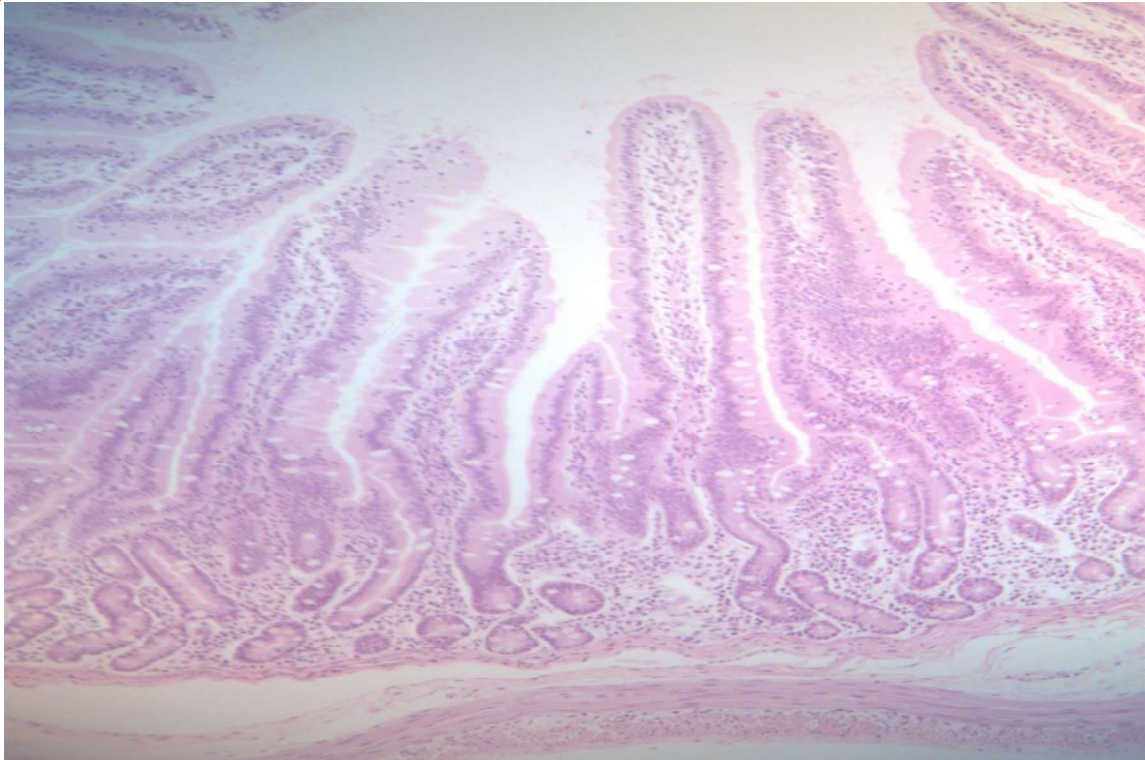
944 B)  
945



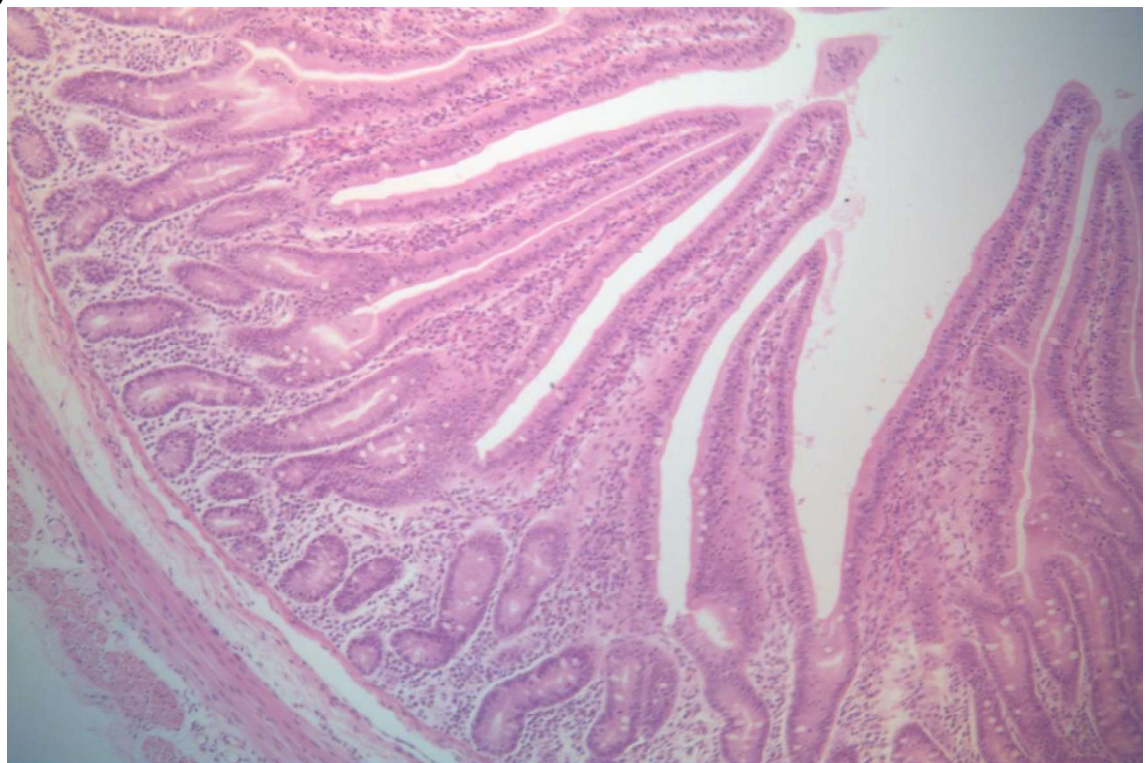
946

947 **Supplementary Figure 3.** Histology images from the duodenum of pigs fed (A) MEM-IMF  
948 or (B) HT-IMF diets for 28 days. Tissue samples from the duodenum were cut into 5  $\mu$ m  
949 sections, mounted on glass microscope slides and stained with haematoxylin and eosin.

950 A)

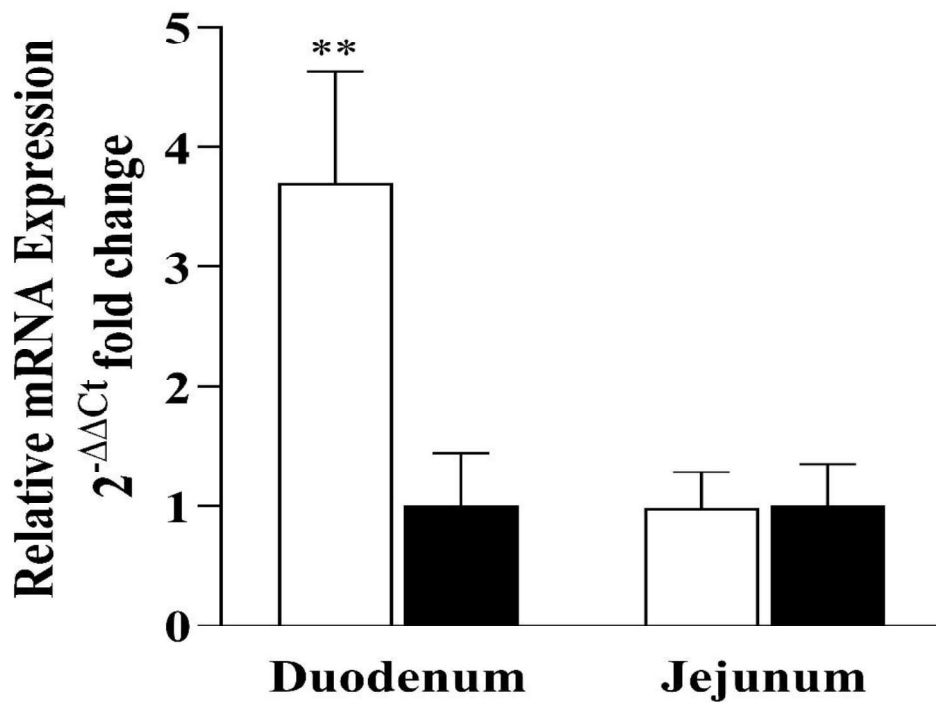


951 B)  
952



953

954 **Supplementary Figure 4.** Histology images from the jejunum of pigs fed (A) MEM-IMF or  
955 (B) HT-IMF diets for 28 days. Tissue samples from the jejunum were cut into 5  $\mu\text{m}$  sections,  
956 mounted on glass microscope slides and stained with haematoxylin and eosin.



957

958 **Supplementary Figure 5.** mRNA transcript levels of *IL-6* in the duodenum and jejunum

959 mucosal scrapings of pigs fed MEM-IMF (white) or HT-IMF (black) diets for 28 days.

960 Mucosal scrapings were collected at slaughter 3 h after final feeding. Values are reported as

961 means  $\pm$  SEM (n = 8 pigs per treatment). The relative quantification of target mRNA was

962 calculated using the reference gene RPLP0 following the  $2^{-\Delta\Delta C_t}$  method. Transcript levels are

963 expressed as the fold change relative to the mean value of the HT-IMF (control) diet.

964 Significant differences between diets for *IL-6* at each gut location are indicated by \*  $P < 0.05$ ,

965 \*\*  $P < 0.01$  and \*\*\*  $P < 0.001$ . *IL-6*, interleukin 6. MEM-IMF = membrane filtered infant

966 milk formula; HT-IMF = high-temperature infant milk formula.